UCRL--15526

DE83 012108

X-RAY SPECTRAL-LINE COINCIDENCES BETWEEN FLUORINE VIII (AND IX) AND TRANSITION-METAL LINES

G. Charatis and P. D. Rockett

KMS Fusion, Inc.

P. G. Burkhalter

Naval Research Laboratory

This work was performed under the auspices of the U. S. Department of Energy under subcontract number 7774001 with Lawrence Livermore National Laboratory and DOE contract number DE-AI08-79DP40092.

KMSF U-1295

X-RAY SPECTRAL-LINE COINCIDENCES BETWEEN FLUORINE VIII (AND IX) AND TRANSITION-METAL LINES

G. Charatis and P. D. Rockett

KMS Fusion, Inc.

and

P. G. Burkhalter

Naval Research Laboratory

ABSTRACT

X-ray spectroscopy was performed in the 12-15 Å region, recording L-shell lines from selected laser-irradiated transition metals in a joint KMS Fusion, Inc.-Naval Research Laboratory, experiment. Line coincidences and near-coincidences were identified between Fe, Cr, Mn, and Ni L-spectra, and F VIII and F IX K-shell lines. Wavelengths were determined to accuracies of 1-3 mÅ and will be utilized in selecting potential pumping candidates in future x-ray lasing schemes. High-resolution x-ray spectra were collected under controlled illumination and target conditions using 1.05 μm and 0.527 μm laser excitation with the KMS CHROMA laser. Laser intensity varied from 1.2-2.5 x 10^{14} W/cm^2 in 200 ps pulses. Three groups of x-ray spectra were collected with highly-dispersive x-ray crystals at wavelengths centered at 12.643, 13.781 and 14.458 Å corresponding to He- and H-like lines from fluorine. Two specially-designed flat-crystal spectrographs employing

camera shutters were used with pairs of beryl and TAP crystals. The spectra from potential lasant and pump candidates could be recorded on the same spectrogram to aid in identifying x-ray line coincidences. In cases where wavelengths were measured in both the 1.05 μm and 0.527 μm laser work, agreement within 1-3 mA was obtained for the L-series x-ray lines. Within this accuracy range, some five L-series x-ray lines, mostly 2p-3d transitions from the metals Cr, Mn, and Ni, had wavelength values coincident with K-series lines in fluorine.

This work was performed under the auspices of the U.S. Department of Energy under subcontract number 7774001 with Lawrence Livermore National Laboratory and DOE contract number DE-AI08-79DP40092.

CONTENTS

I. INTRODUCTION

The use of lasers to drive x-ray lasing transitions has become a serious goal within the national laboratories.[1] Pumping schemes include both collisional excitation and optical pumping to produce population inversions in appropriate elements. The present work at KMSF involved a search for laser-driven spectral lines in the transition metals, which could be used to optically pump lasing transitions in fluorine or neon. This complemented earlier work in this area at LLNL on SHIVA. The results of the KMSF work are to be used in preparing experiments on x-ray laser development on NOVETTE when it becomes operational in early January 1983.

The choices of candidate pump/lasants studied in the KMSF experiments arose from the work by P. L. Hagelstein of LLNL on the physics of short wavelength laser design.[2] From among several population inversion schemes he has examined in detail many resonantly-pumped photo-excitation schemes and has suggested several of these which appear more likely to succeed in providing reasonable gain-producing x-ray laser configurations.

An example of a photo-excitation pumping scheme using He-like neon is shown in Ref. 2 (p. 237). Line radiation at $\lambda \approx 11.547$ Å pumps Ne IX ions from their $1s^2(^1S)$ ground state to the $1s3p(^1P)$ state. De-excitation of the 1s3p state can occur in several ways: (1) back to the ground state or (2), as an example, to the $1s3d(^1P)$ state. If the decay rate of the $1s2p(^1P)$ state is large compared to the decay rate of the 1s3d state, then a population inversion can exist between these two

states, thus making it possible to obtain laser gain. This, in principle, is the scenario for the planned NOVETTE experiments at LLNL.

Photo-excitation, for example, from the $1s^2(^1S)$ ground state of He-like Ne IX can be accomplished (i.e., pumped) by x-ray line radiation from one or more elements with transitions which coincide almost exactly with the $1s^2$-1s3d transition. In fact, it is important that the pump-element line peak is within 1-2 mÅ of the lasant element transition, otherwise the photo-excitation (in this case, $1s^2$-1s3p) will not occur.

In the past decade, a number of spectroscopic studies has been conducted using high temperature plasmas generated by focussed laser beams and vacuum spark sources. Several groups, including those at Goddard, NRL, Culham, Lebedev, Rutherford, Soreq, Lund, and Racah, have made extensive spectroscopic studies to measure the wavelengths of L-shell transitions in metals. Agreement in wavelengths within 1-2 mÅ between two or more laboratories have been rare. Typically, the accuracy quoted has been 5 to 10 mÅ and this is generally the level of agreement in wavelengths, as well. In Ne-like Ni, the disagreement has been as much as 5 mÅ. Clearly, there exists a need to remeasure certain x-ray wavelengths, particularly possible lasant-pump line candidates, under carefully controlled experimental conditions with good spectral dispersion.

Lasant lines with possible pump line counterparts selected initially for the present study were based on published wavelength data, and are shown in Table I. They represent elements which were to be fabricated into targets and irradiated within the time alloted for these experiments.

In the 12-15 Å region, Fe spectra have been most extensively measured and classified. For the other pump elements, atomic structure calculations are required. The wavelengths of the fluorine lines are based on theoretical calculations[2–4] that are believed to be accurate to 1 mÅ. In the 14.458 Å region, values for F-like 2p-3d transitions in Fe have been reported by three laboratories.[5–7] For some of the stronger Fe lines, the agreement is 1-2 mÅ and, therefore, have been used for wavelength calibration and to determine the magnitude of the Doppler shifts associated with the fluorine lines. At 13.781 Å there are not sufficient Fe lines available to be used for calibration purposes. Instead, for the wavelengths reported, Be-like Cr were used; however, the wavelength agreement between two laboratories was only 8 mÅ.[8–9]

In the 12.643 Å region, there exist strong 2p-3s, 3d transitions in Ne-like Ni. The values reported by three groups disagree by as much as 15 mÅ. Two intense Li-like Cr lines, 2s-3p lines of Cr XXII also occur in this region. The values measured for these two lines are nearly in agreement at two different laboratories, but are 7 to 9 mÅ higher than two independent theoretical calculations.[10–13]

Calibration lines were chosen from the literature which were most consistent externally with each other and internally with our data. We then cross-checked the wavelengths obtained in a data set collected with 1.05 μm light to one collected with 0.527 μm laser light.

Experiments were performed and spectra investigated for the fluorine lasant lines and their associated metal line pumps, and they are reported in Section III. The neon lines, however, were not successfully excited, so that direct comparison with associated metal lines was not attempted. However, intercomparisons of three of these

metal pump lines were made. Because of time constraints, we did not investigate the 11.547 Å region.

The experimental plan included the following special features:

(1) laser irradiation was performed with 1.05 μm light, with a subset at 0.527 μm;

(2) short laser pulse lengths were employed, to keep the plasma plume generated as small as possible, yet consistent with sufficient intensity to give useable optical densities on the recording film;

(3) two high-dispersion, high resolution spectrographs were used to record the spectra at two different viewing angles, to account for source broadening and Doppler shifts;

(4) to better observe the line coincidences between the metal pump and lasant spectral lines, appropriate shutters were employed to record the spectra adjacent to one another;

(5) auxiliary lower dispersion spectrographs were used to monitor the progress of the spectral emission of each shot; and

(6) pinhole cameras monitored the x-ray emission of the plasma plumes from shot-to-shot to guard against shifts in laser and target misalignment.

II. EXPERIMENTAL DESIGN

A. Laser-Target Conditions.

The experiments were performed using one beam of the CHROMA I laser, both at 1.05 μm and at 0.527 μm focused with an f/6 lens(*) onto

---

(*) The f/6 lenses are on loan from LLNL.

targets in an evacuated chamber. Provisions were made to monitor the energy on target, the prepulse energy, and far-field and equivalent-plane images, as shown in Figure 1a. Target focusing was accomplished by a TV optical system, both by moving the f/6 lens and the target, using light from an ancillary CW YAG laser at 1.06 μm, or an Ar-ion laser at 0.527 μm, back-reflected from the target. This phase of the experiments was critical since target positioning accuracy was necessary to minimize x-ray wavelength shifts in the adjacent (and/or superimposed) comparison of the spectra from two or three target shots. Using two x-ray pinhole cameras, at 52° and 90° to the laser axis to monitor the plasma plumes of successive shots, the target positions were determined to be reproducible to within 100 μm.

When used at 1.05 μm, the laser delivered 40-100 j on target and about half these values in frequency-doubled operation. Laser pulse duration was varied nominally from 100 to 200 psec, depending on whether superimposed or single shots, respectively, were sufficient to produce measurable spectra on the films. The laser intensity was $\sim 2.5 \times 10^{14}$ W/cm^2 at 1.05 μm and 1.2×10^{14} W/cm^2 at 0.527 μm for 200 psec pulses. The data obtained with the equivalent plane camera system, using an f/6 lens(*) identical to the one employed in focusing the laser light onto the target, is not as yet available for this report. Alternatively, by placing a microscope objective 2 mm downstream from the target focal plane, a photograph was obtained of the intensity distribution pattern in the near-field region, shown in Figure 1b, which was representative of what it would be for the actual target shots.

B. Targets

The targets were fabricated by the Department of Material Sciences at KMSF. Two types were developed: metal films and particle layers. The metal targets were sputtered through masks to thicknesses of ~ 650 A and 450 μm diameter onto ~ 3600 A parylene substrates which, in turn, were supported on aluminum frames with large 2 mm diameter openings (see Figure 2). The fluorine targets were prepared by spraying 5-10 μm teflon particles onto the parylene substrate. Sodium targets were made by evaporating a drop of NaCl-containing water onto the parylene. Five targets of one element per aluminum frame were attached to two other similar frames containing the comparison elements, to form a single composite target holder. This was done in order to insure minimal shifts in target positioning (< 100 μm), for exposures requiring the superposition of more than one target shot, and for the single shot comparison spectra.

C. Spectrographs

Five spectrographs were used to record the spectra. They were placed in a 1-meter diameter vacuum chamber and positioned as shown in Figure 3. Three spectrographs employing convex-curved KAP crystals were used to collect survey spectra that provided information about the intensity and degree of ionization for each shot. The two high-resolution spectrographs used pairs of flat crystals, either beryl (2d=15.95 A) in first order or TAP (2d=25.76 A) in second order. Both types of diffracting crystals were selected because of their high reflectivities and high dispersion properties. The slits on the front of the spectrographs were positioned between 14 to 15 cm from the targets and the target-to-film distance for the flat-crystal

spectrographs was roughly 40 cm depending on the wavelength being measured. The film positions were centered in the back-reflection regions of the spectrographs at Bragg angles of ~ 120° (13.781 Å), 129° (14.458 Å), and 158° (12.644 Å). The flat crystal spectrographs had photographic film shutters positioned in front of the x-ray film, allowing the recording of up to three spectra on each shot series. The spectra were recorded physically adjacent to one another or partially overlapping in order to insure accuracy in wavelength determinations and to observe the line coincidences. The windows of the spectrographs were light-protected with stretched 0.85 μm thick polypropylene coated with 1500 Å of aluminum. In front of each spectrograph a replaceable debris shield with similarly stretched polypropylene was used to protect the windows.

Kodak No-Screen film was used for the survey spectrographs and SB-5 film for the high resolution spectrographs.

D. Other Diagnostics

The reproducibility of the plasma positions for a shot series was monitored by their x-ray images produced by two pinhole cameras on No-Screen film. One camera viewed the target at 90°, the other viewed it at 52°, to the laser axis. The 52° camera was filtered with 50 μm of Be and the 90° camera, by 1 μm of Mylar® and 1500 Å aluminum. As mentioned above, the target positions were generally reproducible to within 100 μm.

A set of K-edge filtered PIN diodes monitored the hard x-ray output of the laser-irradiated targets between 5 keV and 29 keV.

E. Data Collection Methodology

Early in our experimental endeavors we discovered that it was necessary to develop a methodology for data acquisition, in order to insure sufficient intensity of the spectra, and to minimize spectral shifts due to shifts in target positioning. First, a target was positioned with the auxiliary laser beam and the TV monitor at the appropriate distance from the focal plane of the laser beam-focusing lens. The spectrographs were loaded with film and the shutters of the flat crystal spectrographs were set after the spectrographs were positioned in the target chamber. Following a shot, the survey spectrographs were removed and films developed. The flat-crystal spectrographs were not moved during a series of shots. Following a recording of acceptable survey spectra, the shutters were repositioned on the flat-crystal spectrographs and another target moved into place, with only x-y movements of the target stage. With 1.05 μm laser light, a single 200 psec shot on metal targets often provided useable spectra. The fluorine lines required 3 shots of 100 psec pulses to obtain sufficient line intensity. One shot of 500 psec duration produced a plasma plume which was much too large, resulting in unacceptable source broadening of the spectral lines. With 0.527 μm laser light, only metal targets were used, but two shots per element were required to collect readable x-ray intensities because the available laser energy was less.

The recording of suitable spectrograms generally required a full day of between 6 and 8 shots. Each spectral series at a selected wavelength was collected at two different angular positions with the pair of diffraction crystals. Each spectral series was repeated to

insure spectral reproducibility. The wavelengths used for calibration were the fluorine lines and published wavelengths for Fe and Cr lines. The wavelengths for the potential pump lines of interest were determined from two separate experiments. In the 1.05 μm series, the fluorine lines were used for calibration after correcting for Doppler shifts. In the 0.527 μm series, published Fe and Cr wavelengths were used for the 120° and 129° settings using the beryl crystals and both experimental and theoretical values for Li-like Cr lines in the 158° setting employing second-order TAP crystals.

The x-ray line positions were measured and spectral patterns recorded with two separate Grant densitometers. The line positions were read on a comparator incorporating a split image prism system. The positions of the spectral line patterns of metal and of the fluorine calibration lines could each be set independently and read alternately by simply rotating the prism. About twenty spectral patterns were read with the densitometer and calibrated in this manner. Spectral patterns were also processed by scanning with a digitizing Grant densitometer. Digital readings were recorded at every 10 micron interval across the spectral patterns, which were 4 to 7 cm wide. The digital readings were stored on magnetic tape with a PDP-8 computer and processed with a computer program that converts film densities to spectral intensities[14] in the NRL advanced scientific computer. The spectral densities were converted into relative x-ray intensities with known calibration data for SB-5 film[15] and theoretical crystal reflectivities for beryl crystals[16] and calculated values for second order TAP.[17] Rocking curve data for the diffraction crystals have been published by Burek.[18] These spectral scans were used to compare with theoretical calculations using

the Cowan atomic structure program[19] in order to subsequently interpret newly observed transitions such as in Be- and B-like Cr and Mn and the Na- AND Mg-like satellite lines in Ni.

The purpose of this report is to present wavelengths of lines measured as pumping candidates in several of the transition metals. The accuracy of the wavelength determinations is dependent on the quality of the spectral data and the accuracy of the published or theoretical wavelengths used for calibration lines. The precision in measuring the x-ray lines was 1-2 mÅ in the best cases of distinct, narrow lines, and 4-5 mÅ for the weaker or broad lines. The agreement in wavelength values for the candidate lines between the 1.05 μm and 0.527 μm light experiments was found to be 1-3 mÅ with both the beryl and the TAP. The accuracy of the wavelength values is dependent on accepting the accuracy of the published wavelengths.

III. LINE IDENTIFICATIONS

Spectra were collected with both 1.05 μm and 0.527 μm illumination. The spectrograms from the 1.05 μm experiments contained both metal spectra and Doppler-shifted fluorine lines. It was hoped that this would permit direct observation of relative line positions of lasant and potential pump lines. The spectrograms from the 0.527 μm experiments contained spatially adjacent spectra from various metals only. Wavelength identification of some data was determined by digitally processing spectra and comparing observed lines to those from atomic structure calculations. Where calculations proved inaccurate, best experimental data from the literature were used to establish reference line identifications. Films were read on the comparator

densitometer and final wavelength values were determined by comparison of 1.05 μm and 0.527 μm data. Potential pump lines were determined from the wavelength values where line coincidences were found. We will first examine selected spectrograms from the two experiments and interpret the spectral scans. The line coincidences can be selected from a tabulation of the measured wavelengths in Table II.

A. Coincidence with F He_β

Initial investigations were made in the wavelength range of the ^1P He_β transition of F VIII, which occurs at 14.458 Å.[2] Spectra from laser-irradiated Cr, Mn, and Ni were examined for coincidences with this line. The pair of beryl crystals was mounted in the flat crystal spectrographs at angles corresponding to a Bragg $2\theta_B$ angle of 129° for the 14.458 Å lines. Figure 4 shows one spectrogram recording of F and Cr. The F He_β line required three shots at 1.05 μm to record, while the Cr lines were recorded in a single shot. The position of the F He_β line has been Doppler-shifted to 14.464 Å and it occurs in a spectral region with strong B-like Cr XX lines. The theoretical wavelength for F He_β at 14.458 Å occurs between two intense Cr lines and is coincident with a weaker line that can better be seen from densitometer scans. The F lines have broad, asymmetric profiles due to Doppler shifts over a distribution of ion velocities while the x-ray lines from the metal targets are nearly symmetric. The resolving power (including the effect of source broadening), $\lambda/\Delta\lambda$, using the beryl crystals is determined from the single shot metal spectrum to be 1700. The densitometer trace acquired from this spectrogram is shown in Figure 5. The asymmetric F line is shifted by the amount indicated. The Cr line at 14.456 Å is in near coincidence with the theoretical position of the F He_β.

Calibration of these spectra was based upon the identification of the fluorine line positions and dispersion in this region was based upon adjacent iron spectra.

Baseline F and Fe spectra appear in Figure 6. The Doppler-shifted F He_β line is overlapped with weak 2p-3d transitions from F-like Fe XVIII. Several spectrograms were recorded and calibrated to determine the Fe and Doppler-shifted wavelengths. Fluorine-like Fe lines have been measured by three groups, namely, Gordon et al. at Culham,[5] Feldman et al. at NRL,[6] and Boiko et al. at Lebedev.[7] A wavelength agreement of 1-2 mA was found for some nine strong Fe XVIII lines and poorer agreement existed in the comparison for the weaker lines in the three reported measurements. For the spectrograph set at $\phi = 180°$ from the incident laser beam, the F lines had peak positions that were +6 to +8 mA higher than the 14.458 Å value for the F He_β line. The spectrograph is viewing through the target towards the laser beam at an angle $\theta = 120°$. The plasma is seen as a column with a velocity distribution directed as a cone towards the laser and yields a positive wavelength shift. This is consistent with the ion velocity distributions with maximum ion velocities in a cone directed upstream along the laser axis as deduced from the spatial and temporal data collected from laser-produced carbon plasma by Irons, et al.[20] The measured peak line shifts in our data for the F He_β line relative to the iron spectral lines corresponds to ion velocities between 1.2-1.8 x 10^7 cm/sec. The measured shifts in the F He_β line for the spectrograph positioned at $\phi = 126°$ with respect to the laser beam were 3-4 mA , which are consistent with calculated shifts of 3.5-4.7 mA for the velocity distributions determined from the $\phi = 180°$ data. In the

0.527 μm study, the $\phi = 126°$ spectrograph was repositioned to $\phi = 105°$ from the incident laser beam to further reduce the Doppler shifts in the data. The wavelengths determined in the green from the transition metals are based on the assumption that the relative ion velocity distributions produce negligible Doppler shifts. The line profiles were generally sharper for the spectra collected nearer normal to the laser beam. Spectral emission was not observable with the spectrograph positioned at 90° to the laser beam because the target holder blocked the plasma emission viewed by the spectrograph window. Figure 7 shows the densitometer trace for the F He_β line and the Fe XVIII spectral region. The identification of the $2p^5$-$2p^4$3d transitions in Fe XVIII could be made from the overlap of atomic structure calculations with the intensity scans shown in Figure 8. The wavelength region where the F He_β line aligns with the Fe spectrum has several weaker transitions in Fe XVIII.

Spectra were recorded for Cr, Fe, and Mn targets with 0.527 μm irradiation. The spectrogram for these three elements is shown in Figure 9. The relative intensity scans for these three elements are shown in Figure 10. The wavelength position corresponding to the F line at 14.458 Å aligns with a weak Cr line and a Mn line. Atomic structure calculations were performed for B-like Cr XX and Be-like Cr XXI transitions. At a wavelength of 14.458 Å, the lines are solely from B-like Cr and the atomic structure calculations are shown overlapped in Figure 11. Mn atomic structure calculations for $2p^3$-$2p^2$3d transitions in N-like Mn XIX show a possible correspondence to our data in this spectral region as seen in Figure 12. The line coincident with the F line may belong to these transitions but a detailed analysis is needed.

B. Coincidence with F He_γ, λ = 13.781 A

The pair of beryl crystals and the film holders were repositioned to collect spectral data at a Bragg angle of ~ 120°. Spectrograms recorded emissions from F, Cr, and Ni plasmas with 1.05 μm irradiation. Upon examination of the spectrogram shown in Figure 13, one finds that the Doppler-shifted F He_γ and F He_δ lines both align with lines in the spectrum. The shifted F He_γ line is about +14 mA from an intense Cr line. The Doppler-shifted F He_δ line aligns with a Cr line within 0.1 mm, where the dispersion of this spectral region is 0.021 A/mm. The densitometer traces for the F, Cr, and Ni spectra are shown in Figure 14. The strong line in the Ni spectrum is a 2p-3d transition in Ne-like Ni XIX at 13.788 A. 0.527 μm irradiation produced spectra for Cr, Mn, and Fe targets and the spectrogram is shown in Figure 15. This spectrogram was read and calibrated to identify line coincidences and to compare with spectra measured using the Doppler-corrected F line wavelengths. For the Cr line at 13.774 A near the F He_γ line, the wavelength agreement between the IR and green experiments was 1-2 mA. The Ni and Cr lines were found to differ by ±7 mA from the F line while the Mn line appeared as a shoulder to an intense Mn line, and was -4 mA from the F He_γ line. A Cr line was found that had a wavelength +5 mA from the value for F He_δ line. The relative intensity scan for the Cr, Mn, and Fe spectra centered around 13.781 A is shown in Figure 16. Atomic structure calculations for Cr XX and XXI reveal that lines in the 13-14 A region belong mostly to Be-like Cr XXI. Figure 17 shows the Cr XXI calculations in this spectral region.

Atomic structure calculations were performed for Be- and B-like Mn XXII and XXI 2p-3d transitions. The predicted spectra occured mainly between 12.3 and 13.6 Å. Calculations were then performed for C-like Mn XX and are shown overlapping the relative intensity scan in Figure 18. For the region of interest there is good correspondence between theory and experiment, indicating that most lines observed belong to Mn XX transitions.

C. Coincidence with F H_β, λ = 12.644 Å

A pair of TAP crystals was used in second order (2d spacing equal to 12.878 Å) to record spectra centered at 12.644 Å corresponding to the F H_β line. Spectra from Cr, Mn, and Ni were recorded in the high dispersion $2\theta_B$ region equal to 158°. One micron radiation was used to acquire spectra including the fluorine line from teflon targets. Irradiation in the green produced spectra from Cr, where the two intense 2p-3s lines in Li-like Cr XXII would serve as calibration lines. The reflectivity for second order TAP was found to be comparable to that of the beryl crystals. Therefore, metal spectra could be acquired in single shots using 1.05 μm light, while two shots with the green (60% conversion efficiency from IR to green) produced readable spectral patterns.

A spectrogram collected with 1.05 μm illumination is shown in Figure 19 for the F, Mn, and Ni target emissions. The Doppler-shifted F H_β line occurs among a complex of Mn lines and in close alignment with a 2p-3d Ne-like Ni XIX line. The arrow in the spectrogram at 12.644 Å indicates a near coincidence between F H_β and an intense Mn line. Densitometer traces for the three spectra are shown in Figure 20. The F line is seen to align within a complex of overlapping

Mn lines. Spectral identifications for Mn are largely unknown in this wavelength region. Atomic structure calculations have been performed for 2p-3d transitions in Be-like Mn XXII and B-like Mn XXI. The lines observed for Mn near 12.6 Å appear to belong to Be-like Mn XXII; however, the classification of lines would require a detailed interpretation.

The spectrogram collected with 0.527 μm laser light is shown in Figure 21 for Cr and Ni target emissions. The two intense 2s-3p lines in Li-like Cr XXII were used for wavelength determinations in the Ni spectrum. However, there is a considerable disagreement between the reported experimental and theoretical values for these two lines as will be discussed in Section IV. The Ni spectrum is a complex array of overlapping spectral lines as seen in the densitometer trace in Figure 22. This spectral region contains the 2p-3d transitions in Ne-like Ni XIX and their satellites in Na-like Ni XVIII. These satellite features have been identified in previous L-series spectra of Ti XII and Fe XVI.[21] The intense $2p^6$-$2p^5 3d$ (^3D) line in Ne-like Ni XIX may have a wavelength value near the wavelength for F H_β; however, previous experimental values have been reported ranging from 12.641 to 12.656 Å for this line. Atomic structure calculations were performed for 2p-3s transitions in O-like Ni XXI. Figure 23 shows the complex spectral region that exists for Ni from 12.4 to 12.9 Å. The spectral calibration shown in this figure is based on the theoretical values reported for Li-like Cr. An intense Ni line occurs at 12.651 Å that is an overlapping complex due primarily to the 2p-3d transition in Ni XIX and a 3d satellite for a $2p^6 3d$-$2p^5 3d^2$ transition in Na-like Ni XVIII. Lines that occur as shoulders on the central line have wavelength values

of 12.646 and 12.661 Å. These shoulders possibly explain the experimental uncertainties in the previous measurements performed with less spectral resolution than that of the present work.

D. Survey Spectra

Three cylindrical spectrographs were used with convex-curved KAP crystals that allowed collection of the total K spectra from the teflon emission and L-series spectra from the transition metals. The survey spectrographs were used primarily as monitors of the x-ray spectral intensities. Spectral lines were recorded on Kodak No Screen film developed by standard techniques. Spectral data were acquired for the multiple shots on each element. Before changing the shutter positions on the flat crystal spectrographs, the film in the survey spectrographs was developed to insure that sufficient x-ray emission had been accumulated to provide readable spectral lines. The KAP spectrographs recorded x-ray lines to 17 Å by using the thin stretched-polypropylene windows. This is evident upon examination of the fluorine spectra in Figure 24. The fluorine spectrum is similar to one obtained from previous laser work with a 1.05 μm focused beam.[22] The He_α line has a wavelength of value of 16.807 Å. This spectrum for the F K series lines was acquired in 2 shots of 200 psec pulses. Figure 25 shows the Ni L-spectrum acquired in a single, 200 psec shot with 1.05 μm irradiation. Transitions in Ne-like Ni are identifiable by pattern recognition such as the 2p-3s and 2p-3d, 4d lines. The regions covered by the high-dispersive flat crystal spectrographs are indicated in the figure. The need for high-resolution spectra to measure wavelengths of lines is evident.

IV. DISCUSSION

Many important factors have led to achieving wavelength values accurate to 1-3 mÅ in this work. These included the careful selection of experimental conditions and techniques, the use of limited-mass targets, the choice and location of the two types of x-ray spectrographs, the availability of suitable x-ray spectrographs, the availability of suitable x-ray diffraction crystals, and the availability of precision densitometers for careful film measurements. Spectra were obtained with good resolution and dispersion to facilitate high precision in determining wavelength values. Even with good spectrograms, the task of finding line coincidences to 0.1 eV is a difficult one in x-ray spectroscopy, because of the spectral complexity and the difficulty of finding suitable lines with known wavelength values accurate to 1-2 mÅ to use as calibration standards. In addition, one must account for the line shapes due to Doppler motion. In selecting accurate calibration wavelengths, one finds difficulty forwavelength regions where suitable H- and He-like K-series lines are not available.

The spectrograms from the two flat-crystal spectrographs were visually compared for a series of shots. Selected spectrograms were read with the Grant comparator densitometer and calibrated with a least-square polynomial program. A precision of 1-2 mÅ was determined obtainable for the intense, distinct lines from a comparison of wavelengths read from the two spectrographs. The line position of broad, weak, or overlapping line were more difficult to determine accurately.

The x-ray line widths for the experiment were estimated from the dispersion relationship by accounting for the finite target size. With 450 μm targets, the estimated widths were 7-10 mÅ. The actual lines were found to have a width of 9-12 mÅ using the beryl crystals. The increase in width can be accounted for by the addition of the Doppler broadening produced by the hot plasma. For the TAP crystals the estimated lines would have widths 2.7 mÅ for 450 μm targets. The measured profiles were approximately 3 mÅ for the metallic targets. The fluorine lines were always broad and asymmetric due to Doppler motion shifts. The line widths recorded for the fluorine lines were found to be sensitive to the laser pulsewidth and pulsewidth was thus minimized. Little difference was noted between F lines obtained with shots of either 100 or 200 psec. The uncertainty in determining the Doppler shifts from the measured peak centroid was found to be about 1 mÅ. The x-ray lines recorded for the two pair of diffraction crystals were broad, being physically 0.4 to 0.6 mm in size because of the finite plasma size. The lines were read at low magnification with a broad slit on the comparator densitometer. The center of the slit was placed between the two spectral strips and both halves of the Decker optical system were aligned to match the line profile and tilt. This compensated for the slight curvature in the lines due to the Kossel effect. It was determined that the centroids of the lines could be measured to a few tens of microns such that precisions of 1 mÅ or less were obtainable.

Once the line positions were precisely known, the accuracy in the wavelength determination was dependent on knowing accurate calibration lines. The L- and M-series x-ray wavelengths from higher atomic

elements have been based on wavelengths of K-series lines, generally the H- and He-like lines. The wavelengths of K-series transitions have been calculated to a high degree of accuracy. When possible, one tries to use K lines for wavelength calibrations. In this work at high spectral resolution, the number of choices is limited for the narrow spectral regions that were recorded. Therefore, suitable known wavelengths in the L-series were needed. The Ne-like lines in L-series spectra are generally distinct and well-measured. However, the spectral ranges covered in each spectrogram are less than one Angstrom. The only Ne-like lines that occurred in the regions of interest were those of Ni XIX for which a wavelength disagreement exists for published values. Another isoelectronic sequence that has been carefully studied has been the F-like ions. Fortunately, many strong 2p-3d transitions in Fe XVIII exist in the 14.0-14.6 Å region and can be used to calibrate the data collected with beryl at $2\theta_B = 129°$. Three laboratories have measured and classified the 2p-3d transitions in F-like Fe XVIII and their values, for the stronger lines, agree within 1-2 mA. Therefore, these could be used for calibration wavelengths. In the 13.3-14.0 Å region that was recorded with the beryl crystal set at $2\theta_B = 120°$, only a few weak lines from F-like Co XIX occur in this region; therefore, suitable F-like calibration lines were not available near 13.781 Å. For the latter region the choices for calibration lines were to use the Doppler-shifted F lines in the IR experiment and the Be-like Cr lines in the green study.

The F-like FE XVIII spectral patterns were read a number of times from spectrograms collected in the two experiments at the two different angles. The calibration for the intense lines agreed within the 1-

2 mÅ uncertainty found in the published values and the weaker lines near 14.458 Å were measured with a wavelength accuracy of 3 mÅ. It was found that the Doppler-shifted F lines could be determined to a high precision.

V. CONCLUSIONS

The measurement and identification of x-ray wavelengths in L-series spectra from transition metals was achieved to within 1-3 mÅ.

A number of L-series pumping candidates was found that possessed lines coincident with He- or H-like fluorine lines. These appear in Table II. The 12.641 Å line in Be-like Mn XXII is near the value of 12.644 Å for the F H_β line. Two near line coincidences occur in Be-like Cr XXI and F-like Ni XX that match the weak F He_δ. In the vicinity of the F He_β line at 14.458 Å near coincidences occur in B-like Cr XX and N-like MN XIX. These lines coincide with the F He_β line to within 1-2 mÅ.

Mn XIX and Mn XX both show very close coincidences with fluorine K-shell transitions. Mn XIX in particular contained a more distinct line in coincidence with F He_β than did Cr XX. In view of these observations we would recommend the use of Mn as a favored potential pump candidate. The observed L-shell transitions were strong; and one can attempt to pump two different lasing schemes at once.

VI. ACKNOWLEDGEMENTS

We wish to thank Peter Hagelstein and Art Toor of Lawrence Livermore National Laboratory for suggesting the need for conducting this study. We also are grateful to Dennis Matthews of LLNL for

valuable discussions regarding this work. The authors are in debt to the entire crew at KMS Fusion for their support and fortitude in making this a successful effort; in particular, thanks are due Don Slater, Roy Johnson, and Erik Storm. Appreciation goes to David Steinman for his persistence in target fabrication and to Robert Schroeder and David Sullivan for perseverence in the collection of the x-ray data. One of us (P.G.B.) wishes to express gratitude to Barry Kent of the Space and Astrophysics Division at the Rutherford Laboratories for the loan of the valuable beryl crystals that made the experiment possible, and special thanks to Brian Sweeney of Sach Freeman Associates for his diligence in the computer processing of the data. Final thanks go to Lawrence Livermore National Laboratory for their loan of a pair of f/6 lenses used in this experiment.

REFERENCES

1. W. Slivinsky, Seminar at N.R.L. held Sept. 24, 1982. Private communications with A. Toor, D. Matthews, P. Hagelstein of Lawrence Livermore National Laboratories; also, private communication with K. Mitchell of Los Alamos National Laboratory.

2. P. L. Hagelstein, Physics of short wavelength laser design, UCRL-53100, Jan. 1981.

3. J. D. Garcia and J. E. Mack, J.O.S.A. 55, 654 (1965).

4. A. M. Ermolaev, M. Jones and K. J. H. Phillips, Astrophys. Lett. 12, 53-56 (1972).

5. H. Gordon, M. G. Hobby, N. J. Peacock, J. Phys. B13, 1985-1999 (1980).

6. U. Feldman, G. A. Doschek, R. D. Cowan, and L. Cohen, J.O.S.A. 63, 1445-1453 (1973).

7. V. A. Boiko, S. A. Pikuz, A. S. Safronova, and A. Ya. Fayanov, Opt. Spectrosc. 44, 498-499 (1978).

8. N. Spector, A. Zigler, H. Zmora, J. L. Schwob, J.O.S.A. 70, 857-861 (1980).

9. V. A. Boiko, S. A. Pikuz, U. I. Safronova, A. Ya. Faenov, J. Phys. B10, 1253-1263 (1977).

10. E. V. Aglitskii, V. A. Boiko, S. A. Pikuz, and A. Ya. Faenov, Sov. J. Quant. Electron. 4, 956-960 (1975).

11. S. Goldsmith, U. Feldman, L. Oren, and L. Cohen, Astrophys. J. 174, 209-214 (1972).

12. B. Edlen, Physica Scripta 19, 255-257 (1979).

13. U. I. Safronova, J. Quant. Spectrosc. Radiat. Transfer. 1975.

14. R. R. Whitlock, Condensed Matter Physics Branch, N.R.L. wrote the XTLFILM program.

15. L. N. Koppel, "X-ray Calibration of Films," SB-5 and RAR 249 2 in the 0.18-0.93 keV Region, ARACOR Rept. TR-112-08-02, March 1982.

16 R. W. Hayes and B. J. Kent, J. Phys. E: Sci Instrum. 14, 688-692 (1981). Also private communication with B. J. Kent.

17. P. G. Burkhalter, D. B. Brown, and M. Gersten, J. Appl. Phys. 52, 4379-4386 (1981).

18. A. J. Burek, D. M. Barrus, and R. L. Blake, Astrophys. J. 191, 533-543 (1974).

19. R. D. Cowan, J.O.S.A. 58, 808-818 (1968); R. D. Cowan and D. C. Griffin, J.O.S.A. 66, 1010-1014 (1976).

20. F. E. Irons, R. W. P. McWhirter, N. J. Peacock, J. Phys. B5, 1975-1978 (1972).

21. P. G. Burkhalter, L. Cohen, R. D. Cowan, and U. Feldman, J.O.S.A. 69, 1133-1139 (1979).

22. U. Feldman, G. A. Doschek, D. J. Nagel, W. E. Bering, and R. D. Cowan, Astrophys. J. 187, 417-420 (1974).

Table I

Lasant Line		Pump Line		
	λ(A)		Configuration	λ(A)
F He_β	14.458	Fe XVIII (F-like)	$2s^2p^5(^2P_{1/2}) - 2s^2p^4(^1D)3d(^2S_{1/2})$	14.456
F He_γ	13.782	Cr XXI (Be-like)	$2p^2(^3P_2) - 2p3d(^3D_3)$	13.779
		Ni XIX (Ne-like)	$2s^2p(^1S_0) - 2s^2p^5(^2P_{1/2})3s(^1P_1)$	13.779
F H_β	12.643 12.645	Ni XIX (Ne-like)	$2s^2p^6(^1S_0) - 2s^2p^5(^2P_{1/2})3s(^1P_1)$	12.654
		Mn XXII (Be-like)	$2p^2(^1D_2) - 2p3d(^1F_3)$	12.643
		Cr XXII (Li-like)	$2s(^2S_{1/2}) - 3p(^2P_{1/2})$	12.656
Ne He_β	11.547	Ni XXI (O-like)	$2s(^2S_{1/2}) - 3p(^2P_{1/2})$	11.539
		Mn XXIII (Li-like)	$2s(^2S_{1/2}) - 3p(^2P_{3/2})$	11.554
		Co XXII (C-like)	$2sp^3(^5S_0) - 2sp^2(^4P)3d(^5F)$	?
Ne He_γ	11.000	Ni XXII (N-like)	$2s^2p^3(^2D_{5/2}) - 2s^2p^2(^3P)3d(^2F_{7/2})$	11.000
		Na X (He-like)	$1s^2(^1S_0) - 1s2p(^1P_1)$	11.003
		Co XXIII (B-like)	$2sp^2(^4P) - 2sp(^3P)3d(^2D)$	?

Table II

Lasant	λ(A)	Pump Line	λ(A)red	λ(A)gn	Transition
F He_β	14.458	Fe XVIII* (F-like)	14.453[a] 14.469[a]	14.453[a] 14.469[a]	2p-3d 2p-3d
		Cr XX (B-like)	14.458	14.457	2p-3d
		Mn XIX (N-like)		14.458-14.459	2p-3d
F He_γ	13.781	Cr XXI* (Be-like)	13.774	13.775[b]	2p-3d
		Fe XIX (O-like)		13.767	2p-3s
		Mn XX (C-like)		13.794	2p-3d
		Ni XIX (Ne-like)	13.788		2p-3s
F He_δ	13.488	Cr XXI (Be-like)	13.493	13.492	2p-3d
		Ni XX (F-like)	13.491		2p-3s
F H_β	12.644	Ni XIX (Ne-like)	12.655	12.657[c] 12.651[d]	2p-3d
		Mn XXII (Be-like)	12.641		2p-3d
		Cr XXII* (Li-like)		12.662[c] 12.656[d] 12.664[e]	2p-3s 2p-3s 2p-3s

* Transitions used for calibration.

a) Fe XVIII wavelength values from H. Gordon, et al. (1980)

b) An average value for Cr XXI from work of N. Spector, et al. (1980) and V. A. Boiko, et al. (1978).

c) Based on the experimental values for Li-like Cr XXII transition reported by S. Goldsmith, et al. (1972).

d) Based on the theoretical value for Cr XXII from B. Edlen (1979).

e) Experimental value for Cr XXII from E. V. Aglitskii, et al. (1975).

FIGURE CAPTIONS

Figure 1a. Schematic of laser diagnostics.

Figure 1b. Photographic near-field representation of the laser irradiation pattern at the target plane.

Figure 2. Schematic of target types and irradiation.

Figure 3. Configuration of x-ray crystal spectrographs.

Figure 4. Spectrogram recorded from F and Cr emissions with the beryl crystal spectrograph #4 at $2\theta_B = 129°$. The spectra were acquired with 1.05 μm illumination in two 200 psec pulses for Cr and three 100 psec pulses for the teflon target.

Figure 5. Densitometer traces of F and Cr spectra collected with 1.05 μm laser irradiation.

Figure 6. Spectrogram collected from F and Fe emissions with the beryl crystal spectrograph at $2\theta_B = 129°$. Both spectra were acquired in three shots of 100 psec duration using 1.05 μm illumination.

Figure 7. Densitometer traces of F and Fe spectra.

Figure 8. Intensity spectrum of Fe in the 14.0-14.6 A region together with atomic structure calculations for the 2p-3d transitions in F-like Fe XVIII. The theoretical lines have their heights plotted proportional to the theoretical oscillator strengths (gf-values).

Figure 9. Spectrogram recorded from Cr, Fe, and Mn emission with beryl at $2\theta_B = 129°$. The spectra were recorded in two shots, each of 200 psec duration with 0.527 μm laser illumination.

Figure 10. Spectra of Cr, Mn, and Fe in the wavelength region of 14.0-14.6 A.

Figure 11. Cr spectrum together with atomic structure calculations for B-like Cr XX.

Figure 12. Mn spectrum together with atomic structure calculations for N-like Mn XIX.

Figure 13 Spectrogram recorded from F, Cr, and Ni emission with the beryl crystal at $2\theta_B = 120°$. The fluorine spectrum required three shots while the metals were recorded with one shot all at 200 psec with 1.05 μm illumination.

Figure 14. Densitometer traces of F, Cr, and Ni from the spectrogram shown in Figure 13. Line coincidences can be seen with both the F He_γ and F He_δ lines.

Figure 15. Spectrogram recorded from Cr, Fe, and Mn emission with the beryl crystal at $2\theta_B = 120°$. The spectra were recorded with two 200 psec pulses of 0.527 μm light.

Figure 16. Spectra of Cr, Fe, and Mn from the 13.3-14.0 Å region.

Figure 17. Cr spectrum and atomic structure calculations for Be-like Cr XXI.

Figure 18. Mn spectrum and atomic structure calculations for C-like Mn XX.

Figure 19. Spectrogram of F, Mn, and Ni collected with the TAP crystal at $2\theta_B = 158°$. The Mn and Ni spectra required one shot each of 200 psec while the F spectral line was collected in 3 shots of 100 psec using 1.05 μm illumination.

Figure 20. Densitometer traces of the spectrogram shown in Figure 19.

Figure 21. Spectrogram of Cr and Ni collected with the TAP crystal and 0.527 μm illumination.

Figure 22. Spectra of Cr and Ni for spectrogram shown in Figure 21.

Figure 23. Ni spectrum in the 12.4-12.9 Å region together with atomic structure calculations for O-like Ni XXI (top level of theoretical lines), Ne-like Ni XIX (two lines and a weak dot), Na-like Ne XVIII transitions identified by 3d satellites (solid line), 3p satellites (dashed lines), and 3s satellites (dotted lines).

Figure 24. Fluorine spectrogram collected with a curved KAP crystal.

Figure 25. Nickel spectrogram collected with a curved KAP crystal in two shots using 0.527 μm illumination.

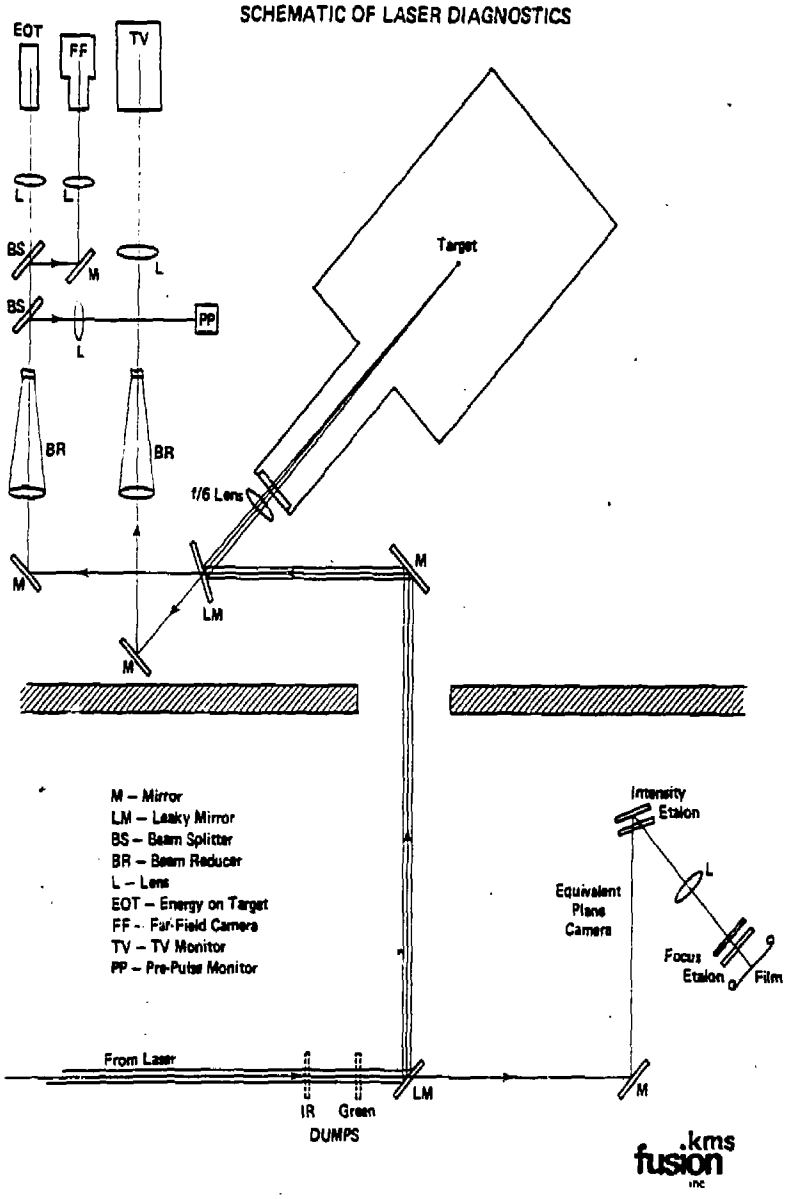
SCHEMATIC OF LASER DIAGNOSTICS
EOT
FF
TV
L
L
BS
M
L
BS
PP
L
BR
BR
Target
f/6 Lens
M
M
LM
M
M – Mirror
LM – Leaky Mirror
BS – Beam Splitter
BR – Beam Reducer
L – Lens
EOT – Energy on Target
FF – Far-Field Camera
TV – TV Monitor
PP – Pre-Pulse Monitor
Intensity Etalon
L
Equivalent Plane Camera
Focus Etalon
Film
From Laser
LM
M
IR
Green
DUMPS
kms fusion inc

Figure 1a

Figure 1b

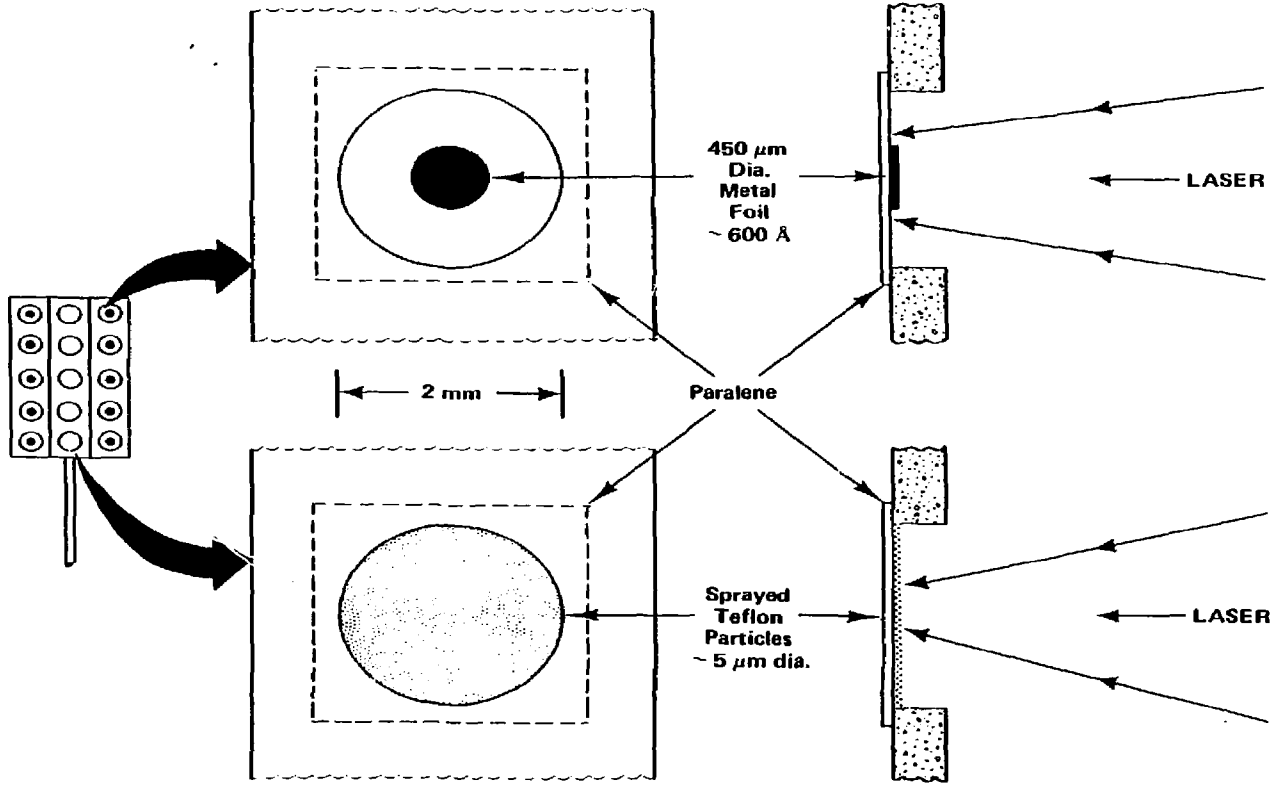

Figure 2 SCHEMATIC OF TARGET TYPES AND IRRADIATION

kms fusion inc

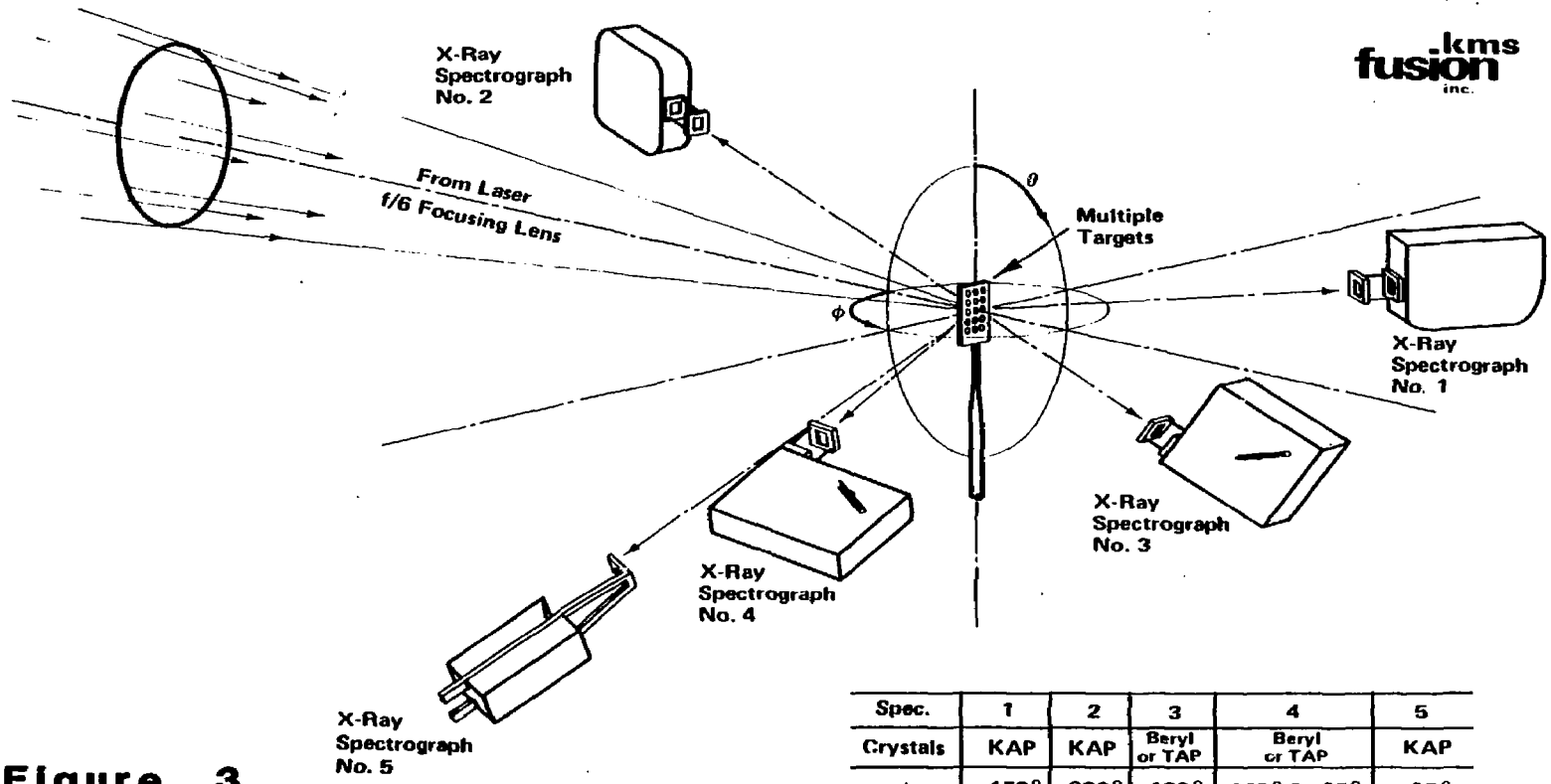

Spec.	1	2	3	4	5
Crystals	KAP	KAP	Beryl or TAP	Beryl or TAP	KAP
ϕ	158°	330°	180°	126° & 95°	95°
θ	90°	90°	125°	90° & 120°	135°
Distance to Film	30.1	30.1	30	25	30 cm

ϕ Measured from laser axis, m horizontal plane
θ Measured from vertical axis through target

Figure 3

SCHEMATIC ARRANGEMENT
OF THE CRYSTAL SPECTROGRAPHS

kms fusion inc.

Spectrograph-4

Beryl 129° First Order

Dispersion: .017 Å/mm

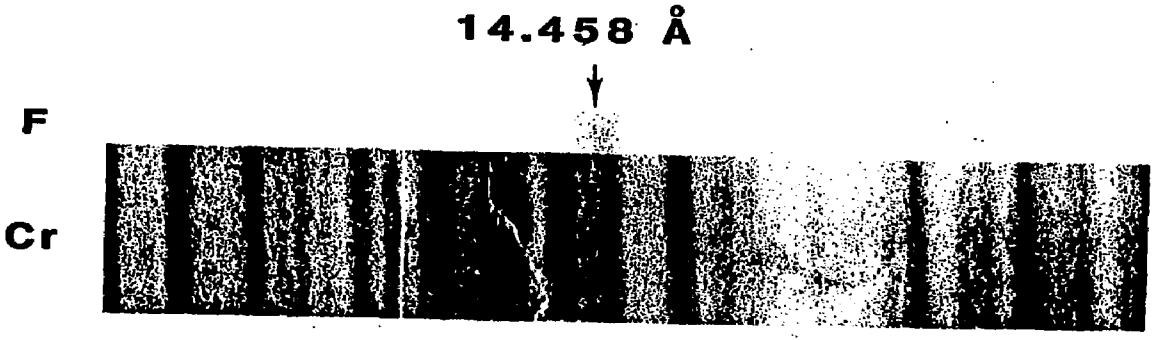

Figure 4

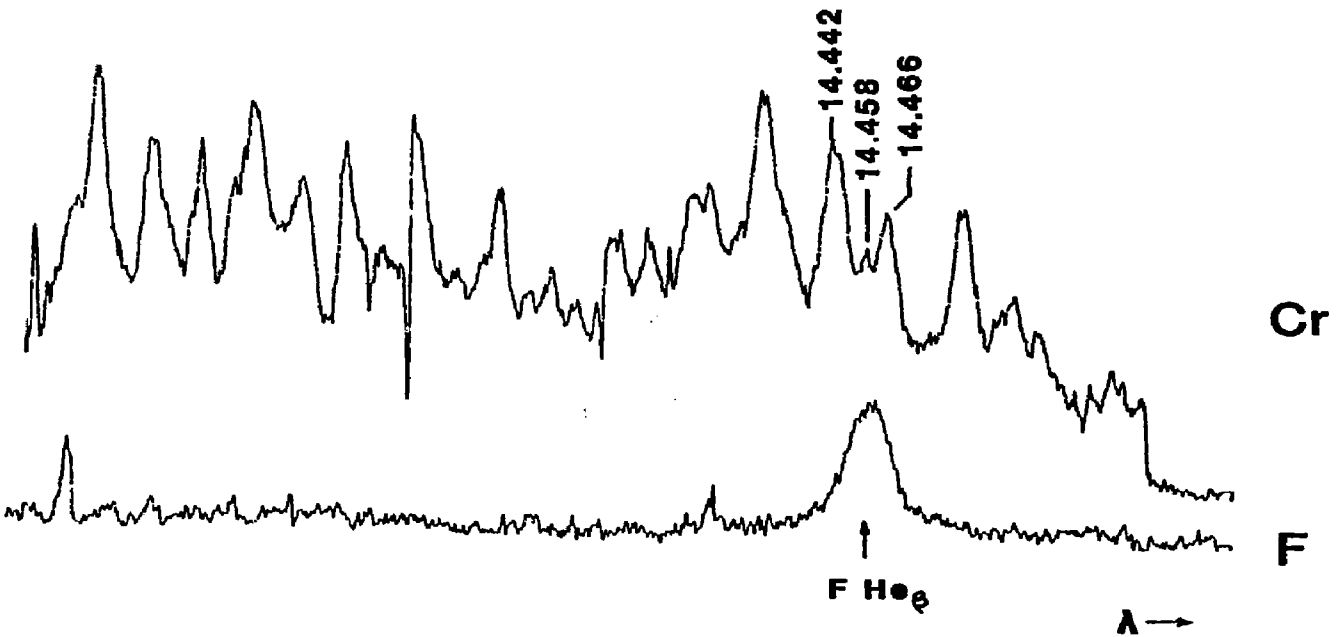

Figure 5

Beryl 129°

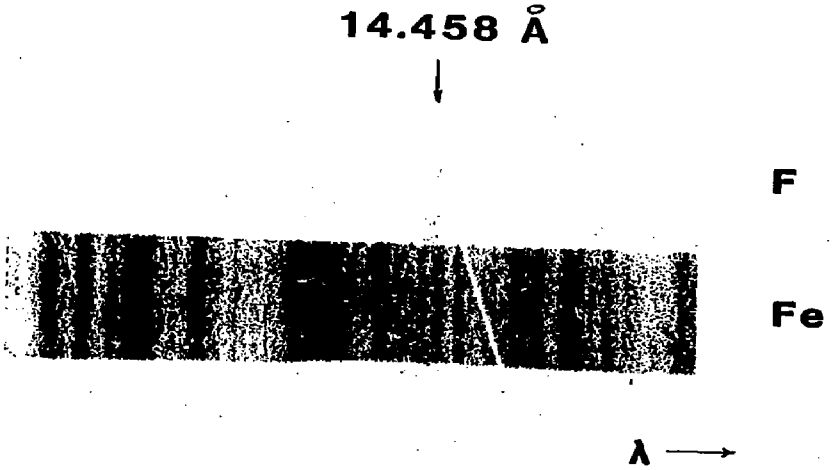

Figure 6

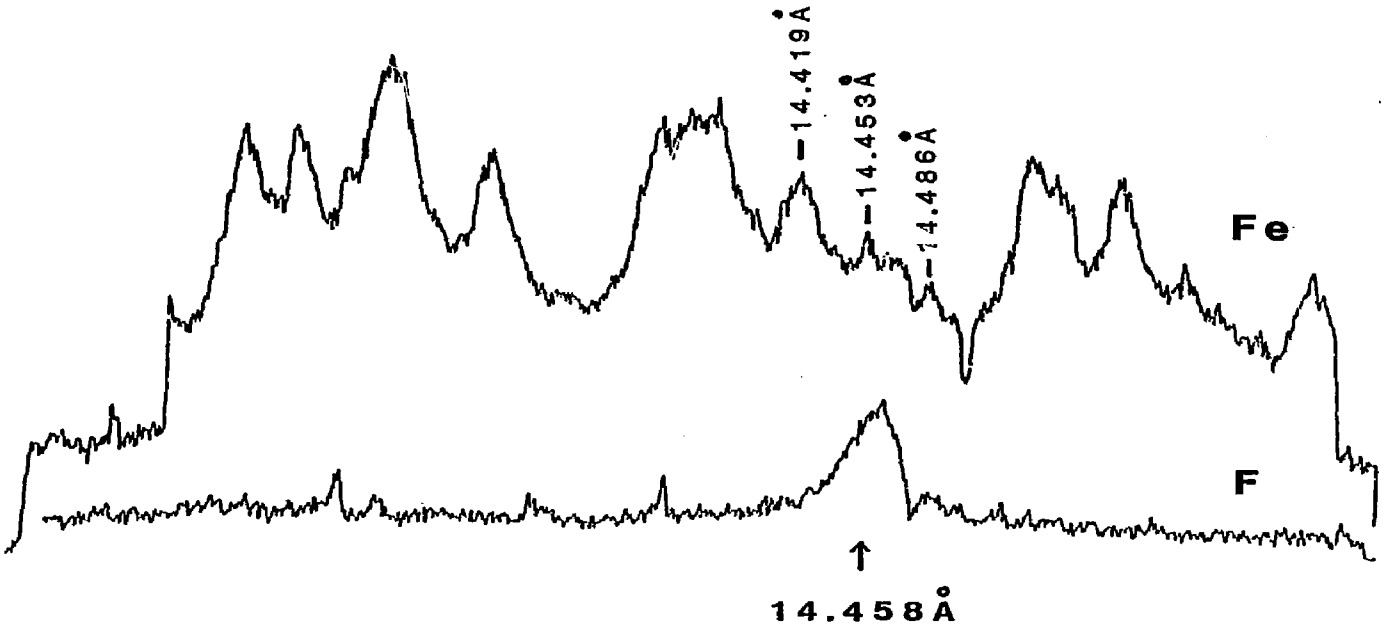

Figure 7

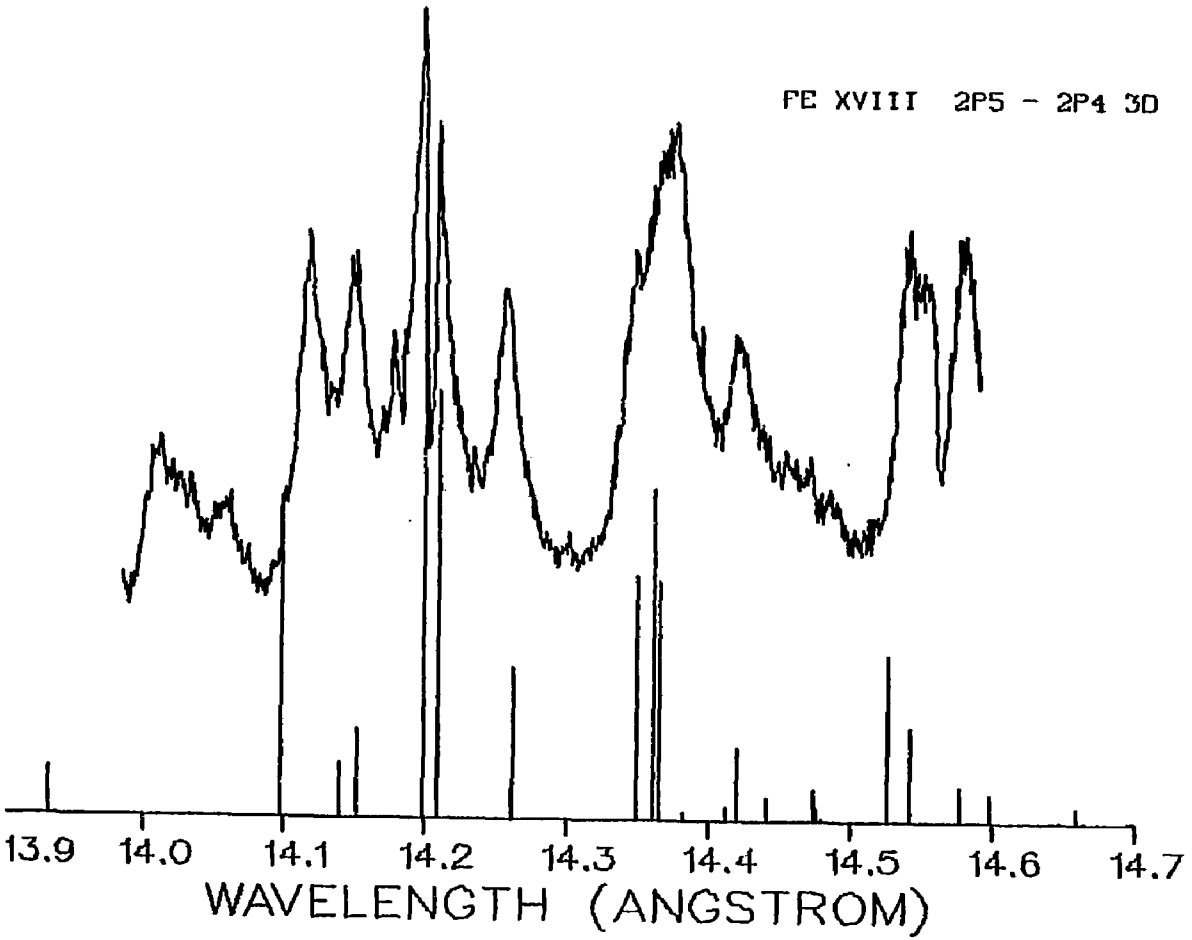
FE XVIII 2P5 - 2P4 3D
13.9
14.0
14.1
14.2
14.3
14.4
14.5
14.6
14.7
WAVELENGTH (ANGSTROM)

Figure 8

Beryl 129°

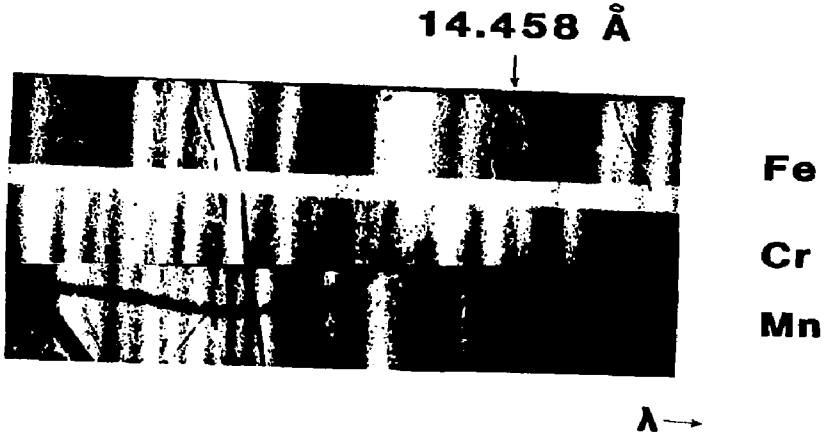

Figure 9

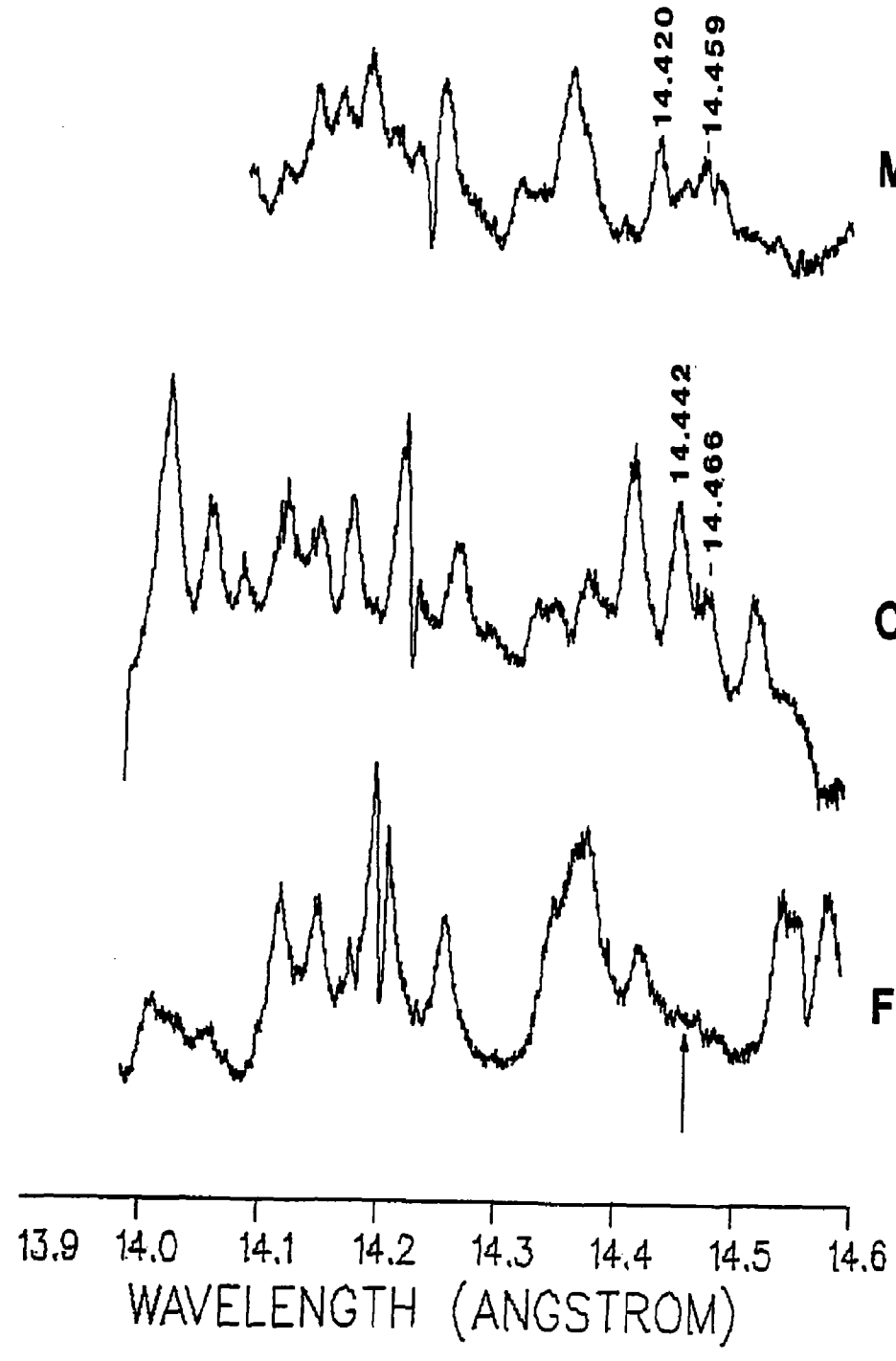
14.420
14.459
Mn
14.442
14.466
Cr
Fe
13.9
14.0
14.1
14.2
14.3
14.4
14.5
14.6
WAVELENGTH (ANGSTROM)

Figure 10

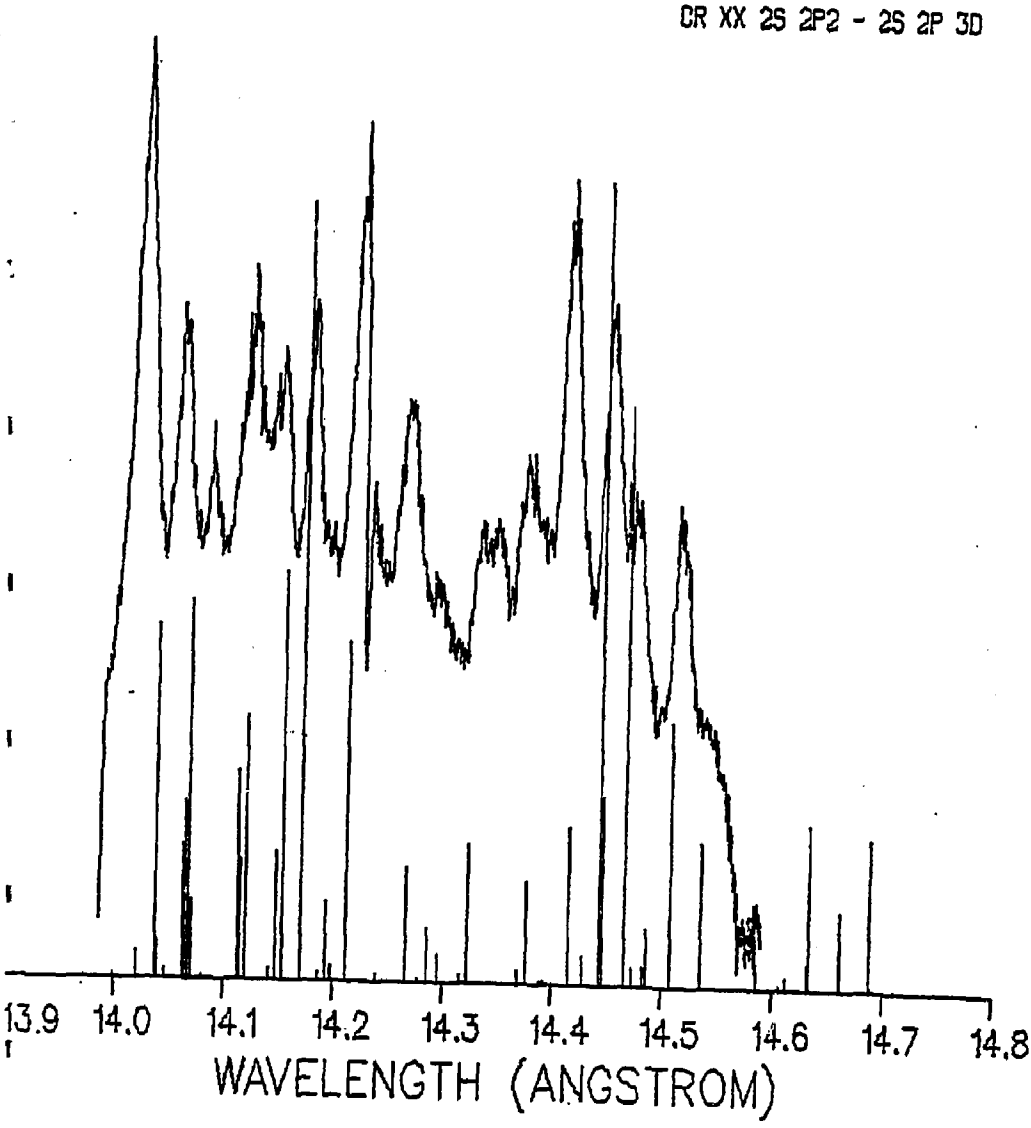
CR XX 2S 2P2 - 2S 2P 3D
13.9
14.0
14.1
14.2
14.3
14.4
14.5
14.6
14.7
14.8
WAVELENGTH (ANGSTROM)

Figure 11

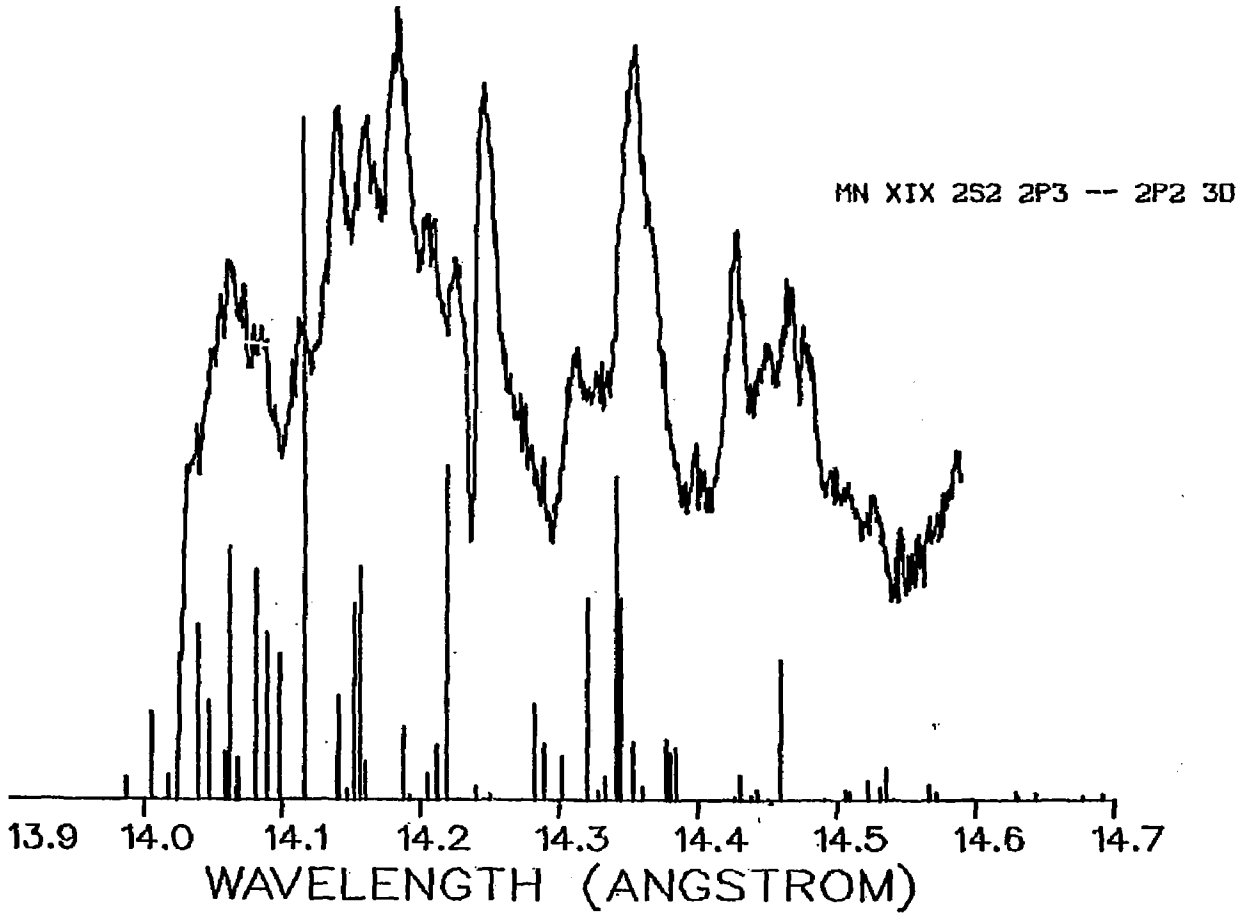
MN XIX 2S2 2P3 -- 2P2 3D
13.9
14.0
14.1
14.2
14.3
14.4
14.5
14.6
14.7
WAVELENGTH (ANGSTROM)

Figure 12

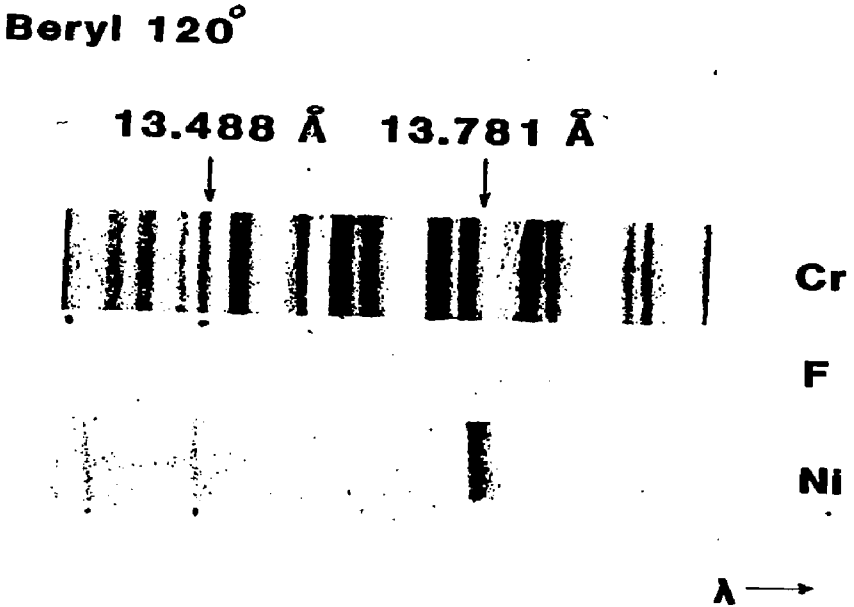

Figure 13

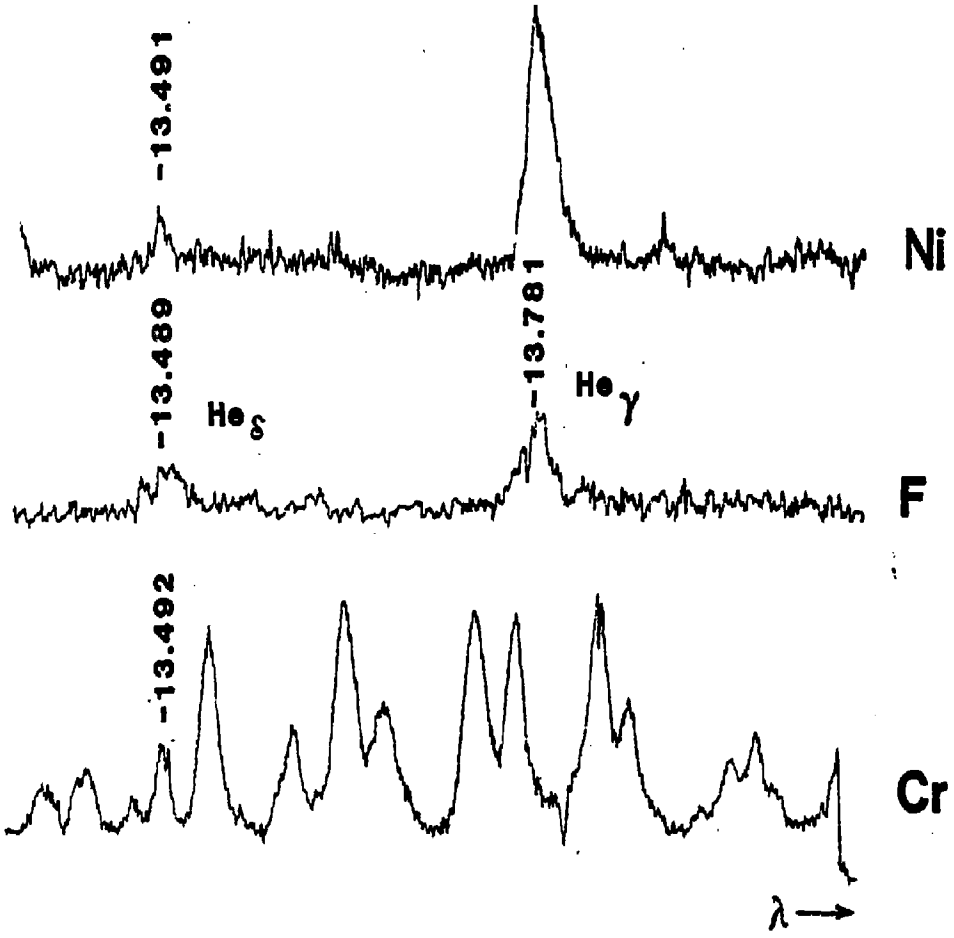

Figure 14

Beryl 120°

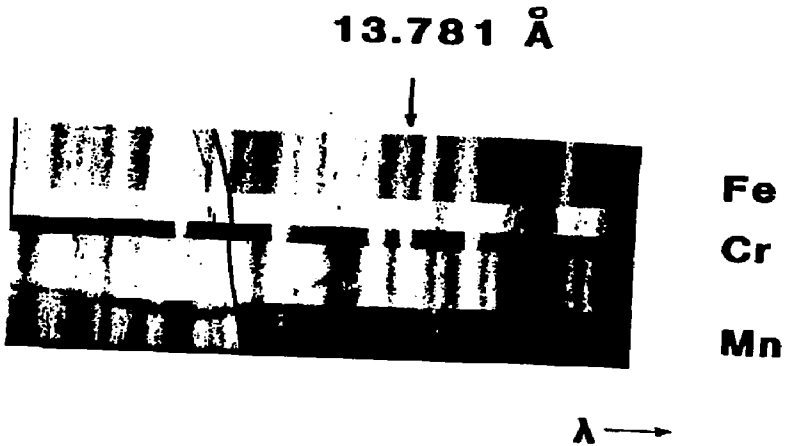

Figure 15

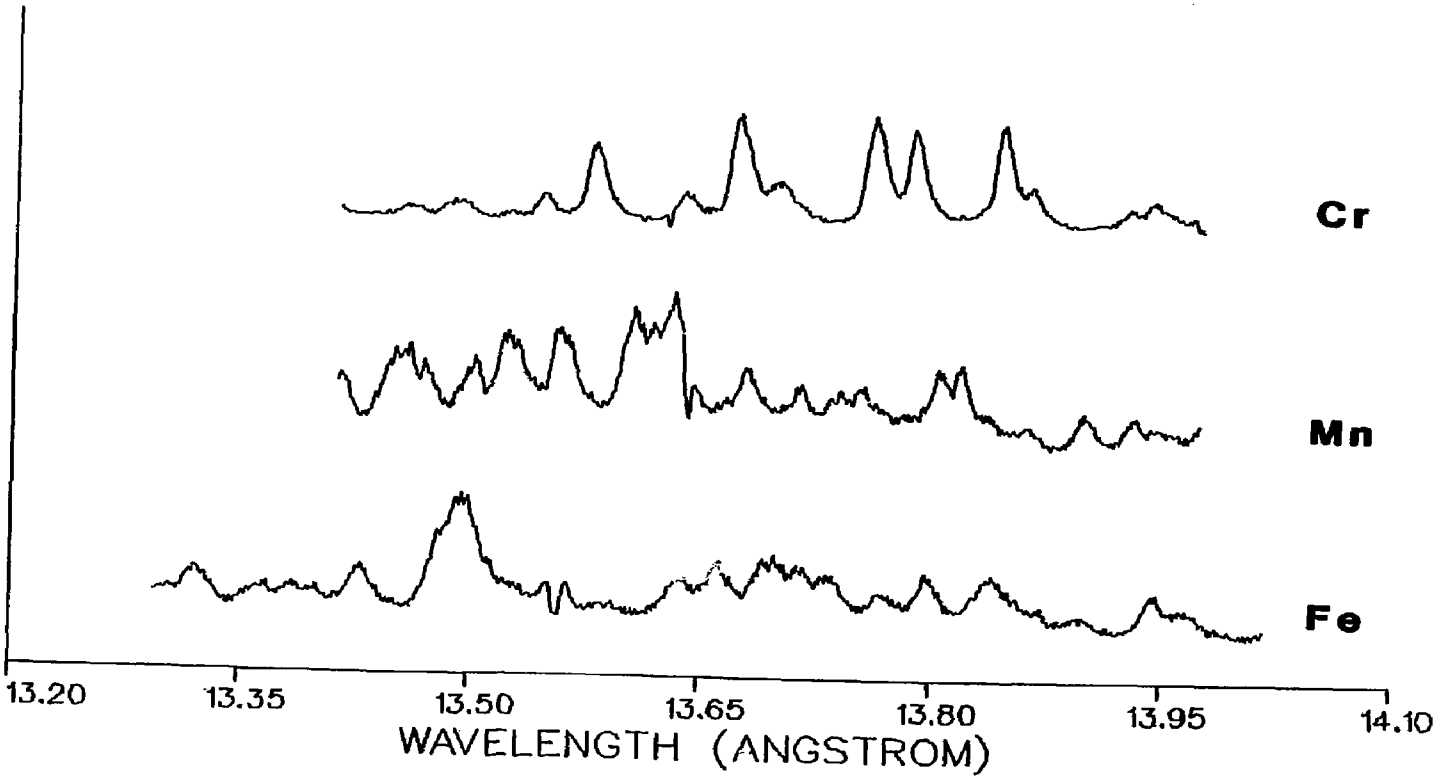
Cr
Mn
Fe
13.20
13.35
13.50
13.65
13.80
13.95
14.10
WAVELENGTH (ANGSTROM)

Figure 16

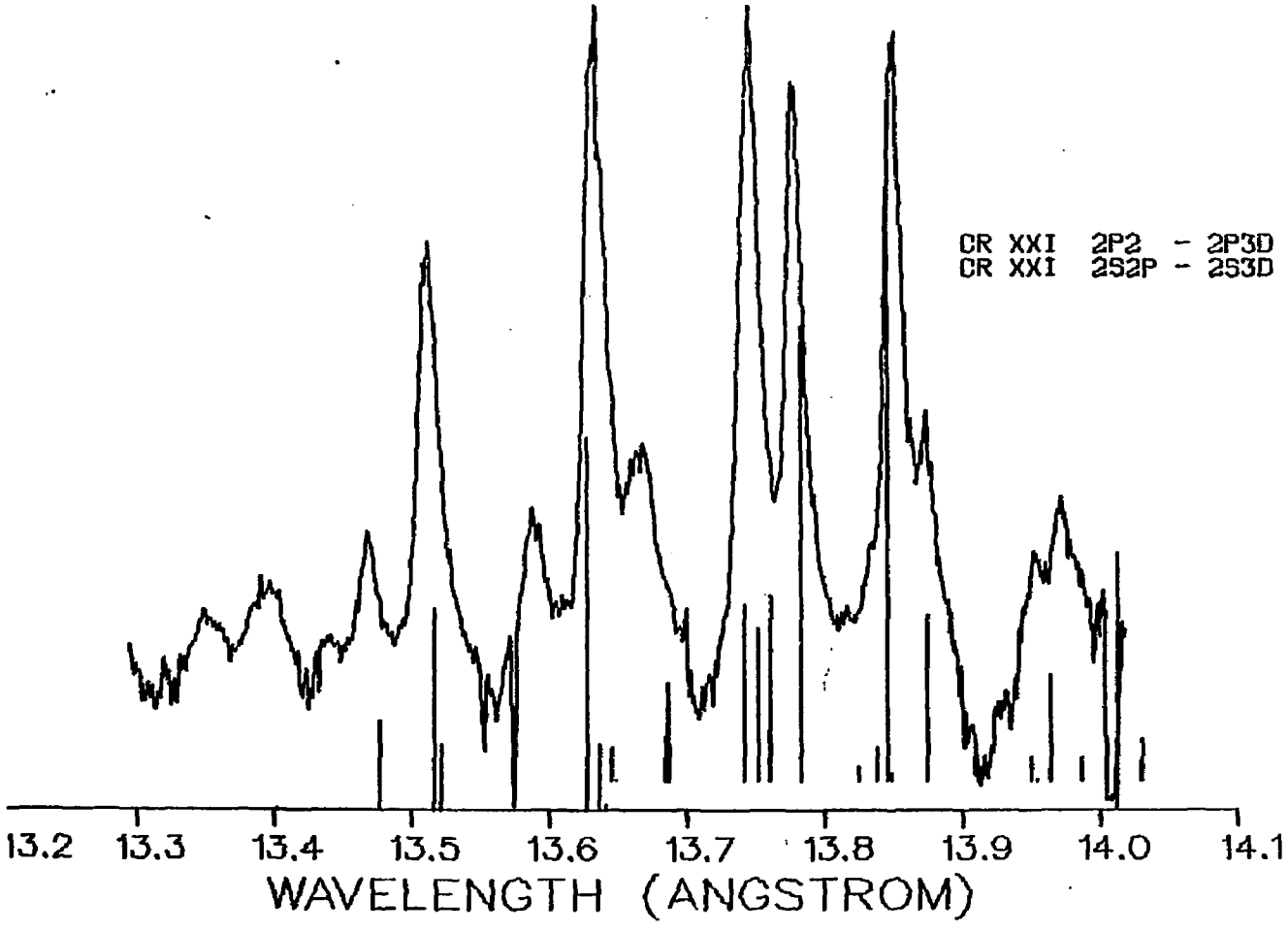
CR XXI 2P2 - 2P3D
CR XXI 2S2P - 2S3D
13.2
13.3
13.4
13.5
13.6
13.7
13.8
13.9
14.0
14.1
WAVELENGTH (ANGSTROM)

Figure 17

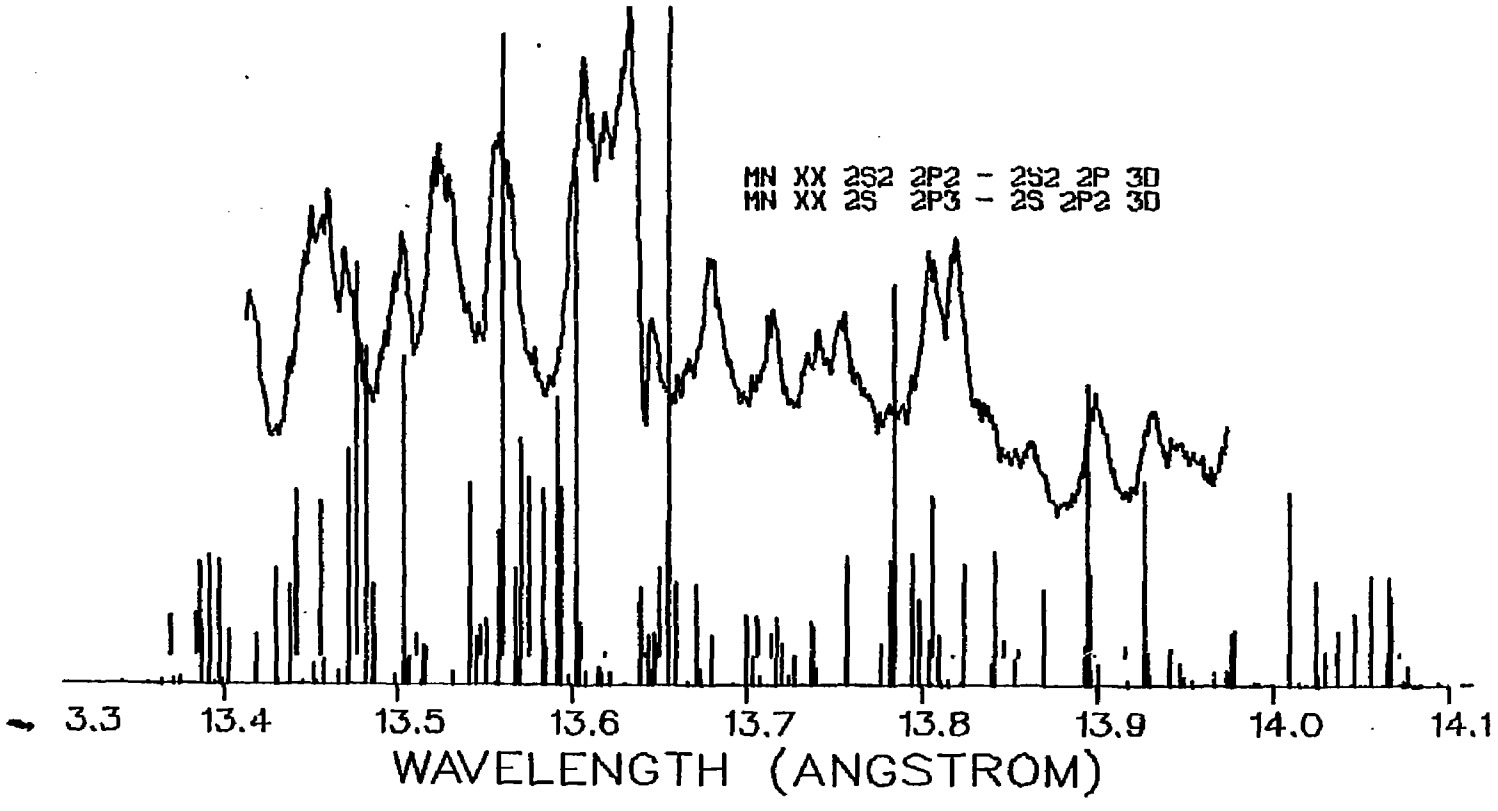
MN XX 2S2 2P2 - 2S2 2P 3D
MN XX 2S 2P3 - 2S 2P2 3D
13.3
13.4
13.5
13.6
13.7
13.8
13.9
14.0
14.1
WAVELENGTH (ANGSTROM)

Figure 18

TAP 158°

Resolving Power Mn:2500

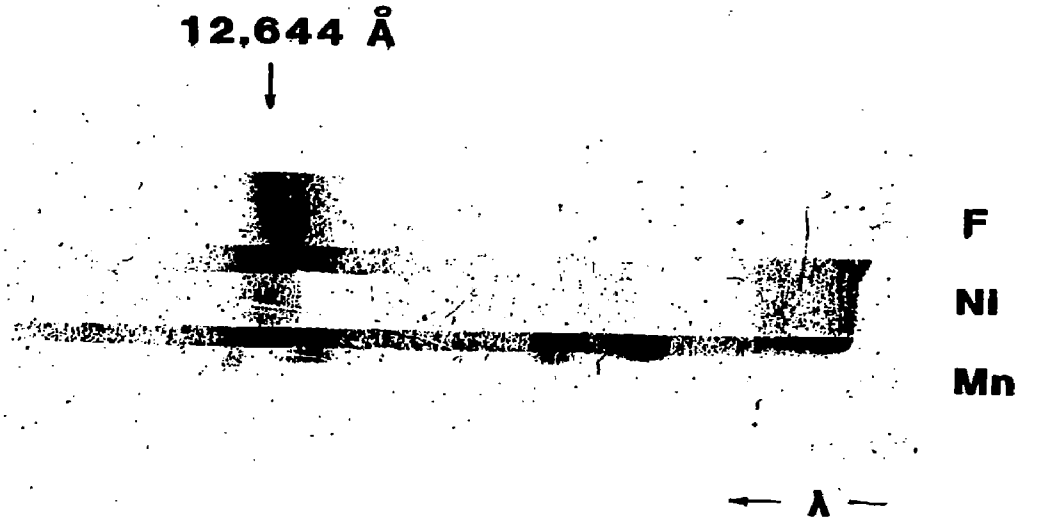

Figure 19

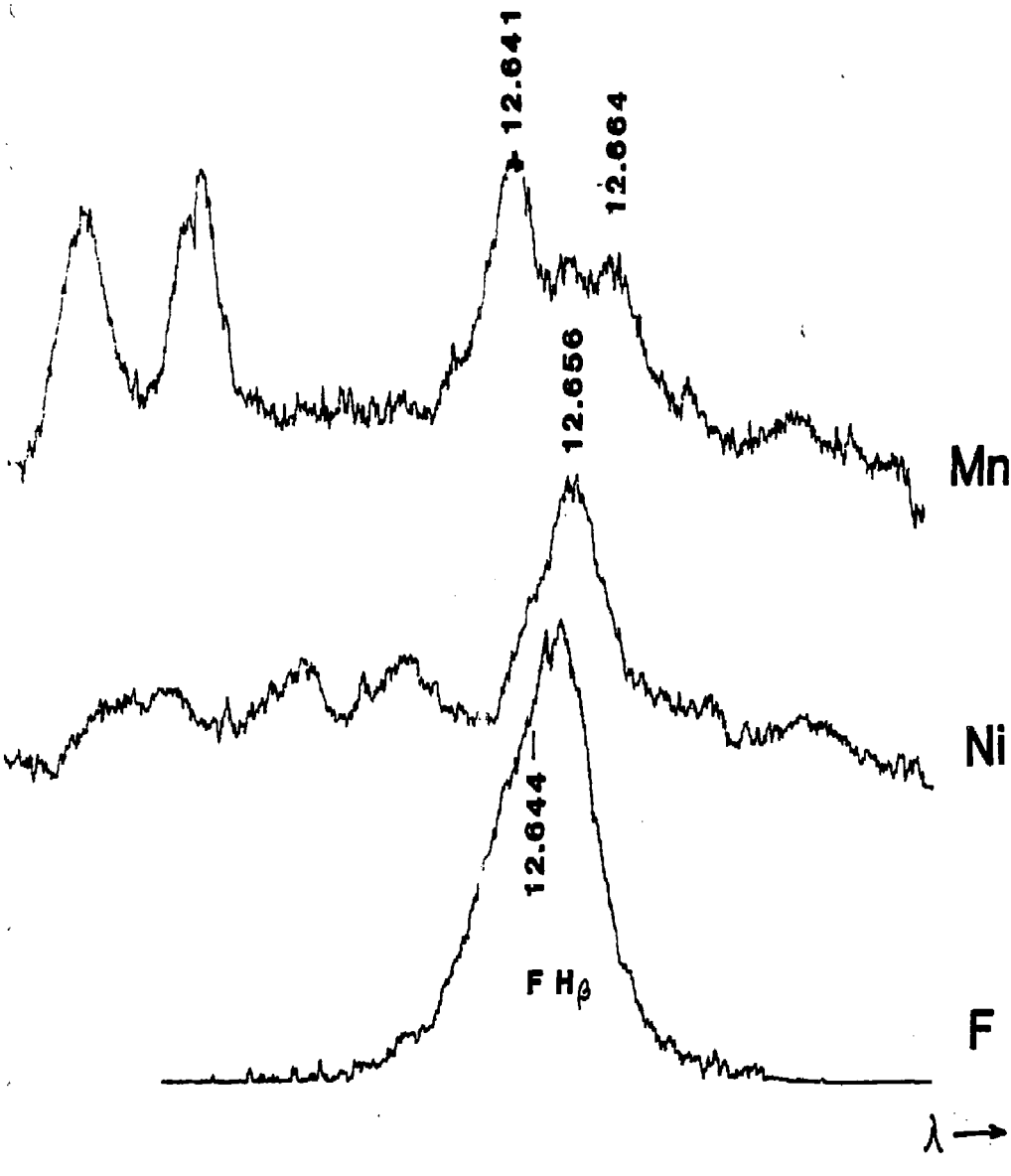

Figure 20

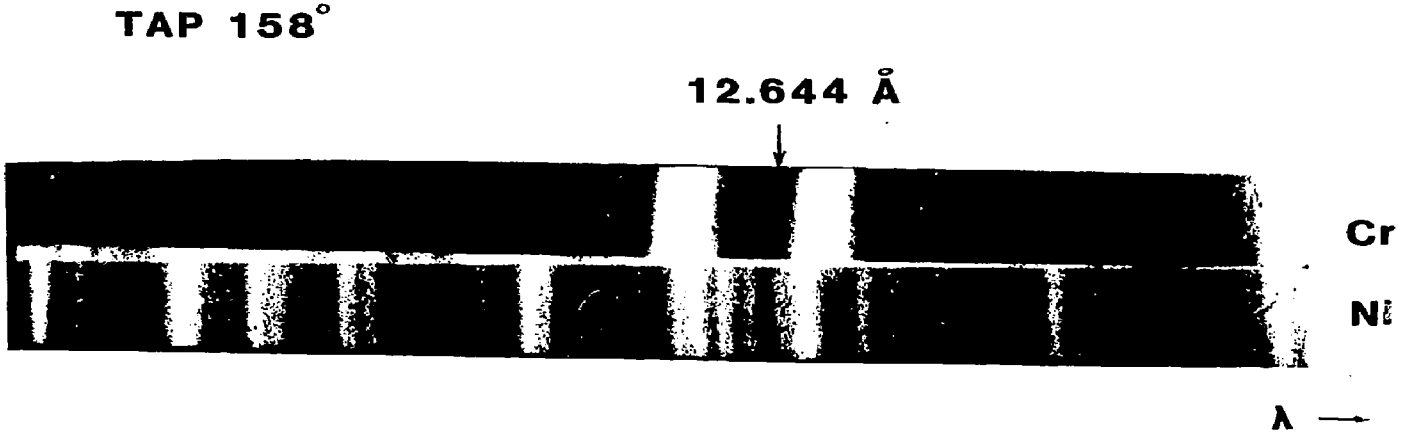

Figure 21

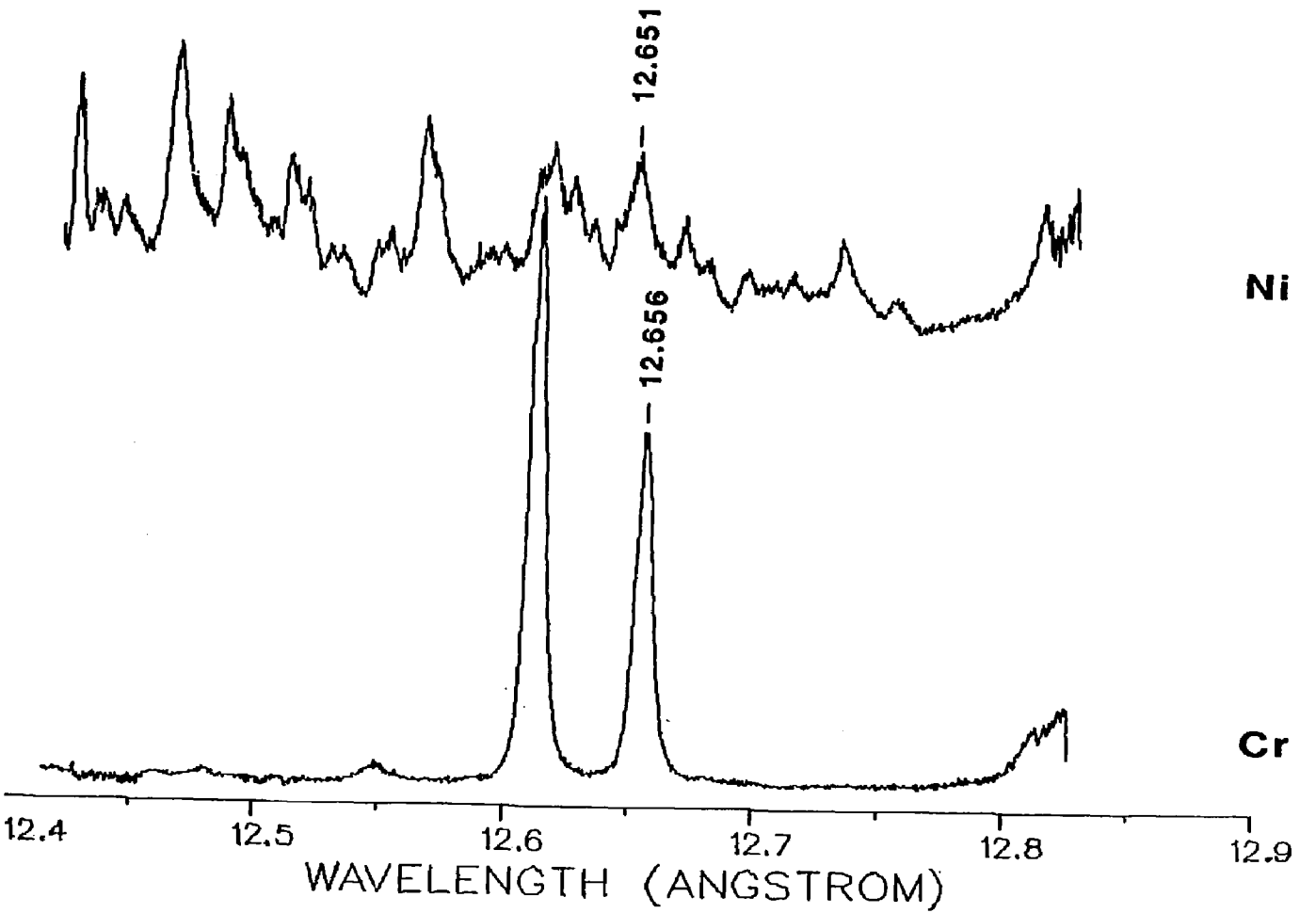
12.651
12.656
Ni
Cr
12.4
12.5
12.6
12.7
12.8
12.9
WAVELENGTH (ANGSTROM)

Figure 22

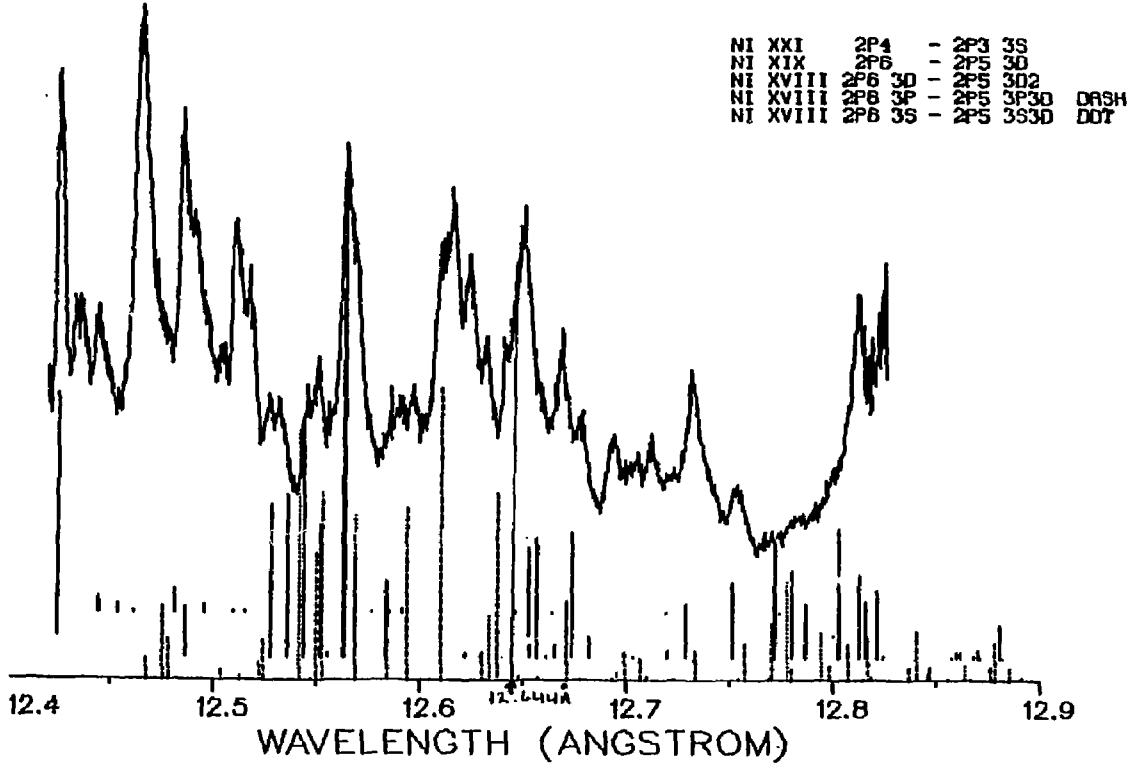
NI XXI 2P4 - 2P3 3S
NI XIX 2P6 - 2P5 3D
NI XVIII 2P6 3D - 2P5 3D2
NI XVIII 2P6 3P - 2P5 3P3D DASH
NI XVIII 2P6 3S - 2P5 3S3D DOT
12.4
12.5
12.6
12.7
12.8
12.9
WAVELENGTH (ANGSTROM)

Figure 23

KAP Spectrograph

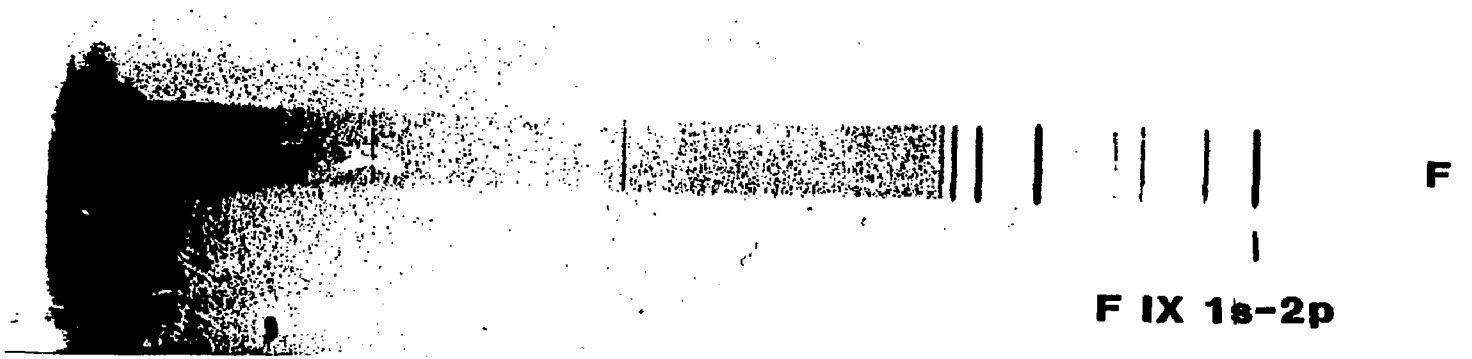

Figure 24

KAP Spectrograph

F H_β at 12.643 Å should coincide with

Figure 25